Cell Reports

Article

A type III-Dv CRISPR-Cas system is controlled by the transcription factor RpaB and interacts with the DEAD-box RNA helicase CrhR

Graphical abstract

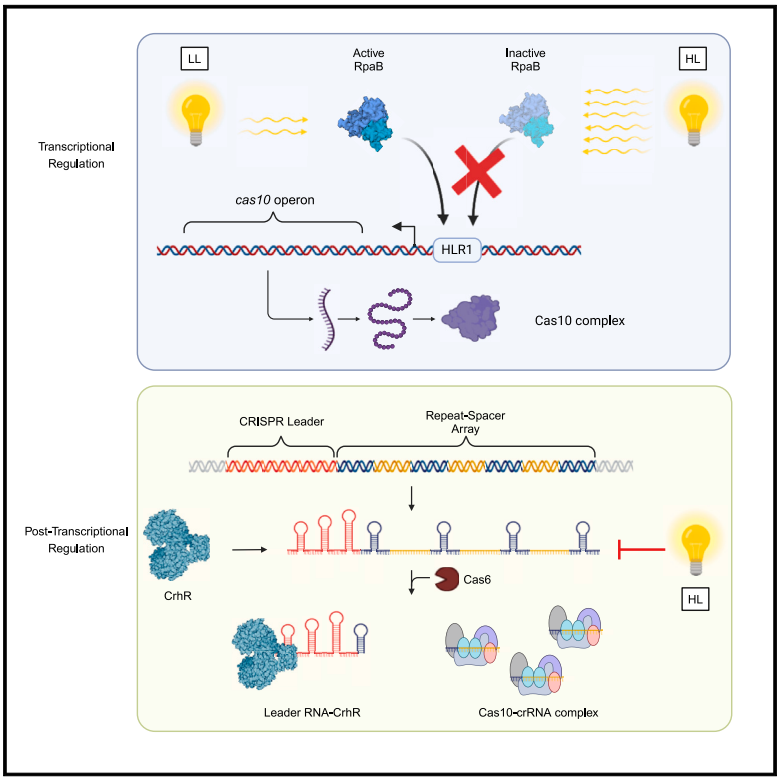

Authors

Raphael Bilger, Angela Migur, Alexander Wulf, Claudia Steglich, Henning Urlaub, Wolfgang R. Hess

Correspondence

wolfgang.hess@biologie.uni-freiburg.de

In brief

Bilger et al. show that, in the cyanobacterium *Synechocystis*, the transcription factor RpaB positively regulates *cas* gene transcription under low light. The CRISPR leader transcript is bound by the DEAD-box helicase CrhR. Both proteins are redox regulated and jointly control the CRISPR III-Dv system at the transcriptional and post-transcriptional levels.

Highlights

- RpaB positively regulates CRISPR III-Dv *cas* transcription in *Synechocystis* 6803
- The RNA helicase CrhR specifically binds to the III-Dv CRISPR leader transcript
- Redox conditions regulate CRISPR/*cas* expression in a photosynthetic cyanobacterium
- Control of a CRISPR/*cas* system by RpaB and CrhR highlights the regulatory complexity

Bilger et al., 2024, Cell Reports *43*, 114485
July 23, 2024
https://doi.org/10.1016/j.celrep.2024.114485

CellPress

Cell Reports

CellPress
OPEN ACCESS

Article

A type III-Dv CRISPR-Cas system is controlled by the transcription factor RpaB and interacts with the DEAD-box RNA helicase CrhR

Raphael Bilger,[1] Angela Migur,[1,4] Alexander Wulf,[2,3] Claudia Steglich,[1] Henning Urlaub,[2,3] and Wolfgang R. Hess[1,5,*]
[1]Faculty of Biology, Genetics and Experimental Bioinformatics, University of Freiburg, Schänzlestrasse 1, 79104 Freiburg, Germany
[2]Bioanalytics Research Group, Department of Clinical Chemistry, University Medical Centre, 37075 Göttingen, Germany
[3]Bioanalytical Mass Spectrometry Group, Max Planck Institute for Biophysical Chemistry, 37077 Göttingen, Germany
[4]Present address: RNA Synthetic Biology Group, Helmholtz Institute for RNA-based Infection Research (HIRI), 97080, Würzburg, Germany
[5]Lead contact
*Correspondence: wolfgang.hess@biologie.uni-freiburg.de
https://doi.org/10.1016/j.celrep.2024.114485

SUMMARY

How CRISPR-Cas systems defend bacteria and archaea against invading genetic elements is well understood, but less is known about their regulation. In the cyanobacterium *Synechocystis* sp. PCC 6803, the expression of one of the three different CRISPR-Cas systems responds to changes in environmental conditions. The *cas* operon promoter of this system is controlled by the light- and redox-responsive transcription factor RpaB binding to an HLR1 motif, resulting in transcriptional activation at low light intensities. However, the strong promoter that drives transcription of the cognate repeat-spacer array is not controlled by RpaB. Instead, the leader transcript is bound by the redox-sensitive RNA helicase CrhR. Crosslinking coupled with mass spectrometry analysis and site-directed mutagenesis revealed six residues involved in the CrhR-RNA interaction, with C371 being critically important. Thus, the expression of a type III-Dv CRISPR-Cas system is linked to the redox status of the photosynthetic cell at the transcriptional and post-transcriptional levels.

INTRODUCTION

CRISPR-Cas systems encode RNA-based adaptive and inheritable immune systems in many archaea and bacteria.[1,2] These systems are highly diverse and were classified into 2 classes, 6 types and 33 subtypes[3]; however, new subtypes are still being discovered. Type III CRISPR-Cas systems, characterized by the presence of the signature gene *cas10*, exist in 34% and 25% of the archaeal and bacterial genomes that encode CRISPR-Cas loci, respectively.[4] Type III systems are further classified into five subtypes, A to E.[3,5,6] Although detailed insights have been gained into the different types of CRISPR-Cas systems, knowledge of how their expression is regulated remains incomplete.

In the subtype I-E system of *E. coli*, regulation by transcription factors has been demonstrated. The DNA-binding protein HNS (histone-like nucleoid structuring protein) acts as a repressor by inhibiting the expression of crRNA and *cas* genes.[7] As an antagonist of HNS, LeuO activates the expression of *cas* genes, thereby enhancing resistance against invading DNA.[8] Finally, a signaling cascade involving the BaeSR two-component regulatory system, which senses envelope stress (e.g., phage attack) via the membrane-localized kinase BaeS, was identified. Once activated, BaeS phosphorylates the cytoplasmic transcription factor BaeR,[9] which, among other genes, activates the expression of *cas* genes.[10]

In the thermophilic archaeon *Sulfolobus islandicus*, expression of the type I-A CRISPR locus is regulated by Csa3a and Csa3b, two transcriptional regulators containing CARF and HTH domains. While Csa3a activates the expression of adaptation genes and CRISPR array,[11] interference genes are repressed by Csa3b. Repression is achieved in the absence of viral infection by cobinding of the cascade complex.[12] In *Serratia*, the LysR-type transcriptional regulator PigU controls the expression of a type III-A and a type I-F system.[13] Further regulatory mechanisms have been described for CRISPR-Cas systems in *Pectobacterium atrosepticum*[14] and *Pseudomonas aeruginosa*.[15,16]

Cyanobacteria are the only prokaryotes whose physiology is based on oxygenic photosynthesis, which makes them immensely important primary producers. Field studies have shown that both cyanobacterial cell counts and the number of co-infecting bacteriophages (cyanophages) can be very high, with up to 50% of all cyanobacteria estimated to be infected at any one time,[17] which likely affects cyanobacterial biogeography and biogeochemistry at the scale of oceanic subregions.[18] Accordingly, active defense mechanisms can be expected in cyanobacteria.

The unicellular cyanobacterium *Synechocystis* sp. PCC 6803 (hereafter *Synechocystis* 6803) is a model for CRISPR biology in cyanobacteria. It possesses three separate CRISPR-Cas systems, a type I-D (CRISPR1), III-Dv (CRISPR2), and III-Bv

(CRISPR3) system, which are highly expressed under a variety of conditions and active in interference assays.[3,19–25] The CRISPR2 system is of particular interest because it has recently been suggested to function as a protein-assisted ribozyme.[24]

Each of the three CRISPR-Cas loci in *Synechocystis* 6803 is associated with one gene that has been suggested to encode a regulator (*sll7009*, *sll7062*, and *sll7078*[25]). Indeed, deletion of *sll7009*, which encodes a putative WYL domain protein, led to increased accumulation of crRNAs in the CRISPR1 system, but did not change the crRNA levels in the other two systems.[26] This result was consistent with the observation that CARF and WYL domain regulatory proteins are widely distributed ligand-binding regulators of CRISPR-Cas systems.[27] Sll7062 differs from the other two possible regulators by the presence of an N-terminal CARF7 family domain fused to a RelE RNase domain, a setup characteristic of Csm6 proteins. Csm6 proteins are not transcription factors but rather CRISPR-associated RNases that are activated by cyclic oligoadenylate-mediated signaling.[28] Accordingly, Sll7062 was renamed SyCsm6 when its activity was tested together with the CARF-HEPN domain protein SyCsx1 (Slr7061).[29] Therefore, the CRISPR2 system lacks an obvious candidate regulatory gene in its vicinity.

However, when we characterized the regulon controlled by the transcription factor RpaB in *Synechocystis* 6803, we noted the possible involvement of a host genome-encoded factor in CRISPR2 regulation.[30] RpaB ("regulator of phycobilisome association B," Slr0947) is an OmpR-type transcription factor that is predicted to control more than 150 promoters by binding to the HLR1 ("high light regulatory 1") motif, a pair of imperfect 8-nt long direct repeats (G/T)TTACA(T/A)(T/A) separated by two random nucleotides. RpaB mediates transcriptional activation when the HLR1 motif is located 45–66 nt upstream of the transcription start site (TSS), whereas other locations mediate repression.[30] RpaB is a transcription factor of central importance for the light- and redox-dependent remodeling of the photosynthetic apparatus and many associated pathways. Surprisingly, there was also a predicted binding site in the promoter that drives the transcription of the CRISPR2 *cas* operon, but this was not investigated further.[30]

Another protein with a central role in light- and redox-dependent responses in *Synechocystis* 6803 is the cyanobacterial RNA helicase Redox (CrhR).[31] CrhR (Slr0083) is the only DEAD-box RNA helicase in *Synechocystis* 6803 capable of altering RNA secondary structures by catalyzing both double-stranded RNA unwinding and annealing.[32] The molecular effects of *crhR* deletion or inactivation have been studied at the transcriptome[33,34] and proteome levels,[35] and several attempts have been made to identify the RNA targets of CrhR directly.[36]

Here, we applied a further approach to pull down RNA that interacts with CrhR, which is expressed as a recombinant protein, and found that the transcribed leader of the type III-Dv CRISPR-Cas system was copurified. Therefore, we investigated the possible regulatory impact of the host genome-encoded transcription factor RpaB on CRISPR2 system expression and described and validated the interaction of CrhR with its repeat-spacer array leader transcript.

RESULTS

The expression of the type III-Dv CRISPR2 system in *Synechocystis* 6803 is affected by environmental conditions

In our previous analysis of the distribution of putative HLR1 binding sites for the transcription factor RpaB in *Synechocystis* 6803, one site was predicted in the CRISPR2 *cas* gene promoter; however, this site has not been studied further.[30] This promoter drives the transcription of six genes, *sll7067-sll7062*, into a single transcriptional unit (TU).[37] Therefore, these six genes constitute an operon. These genes encode Cas10, a Cas7-Cas5-Cas11 fusion, Cas7-2x, Csx19, Cas7 with an insertion, and SyCsm6 (Figure 1A). Technically, two TUs, TU7058 and TU7063, were defined for the CRISPR2 *cas10* promoter because they contain two TSSs (at positions 62704 and 62807 on the reverse strand).[37] Our previous genome-wide mapping of TSSs using differential RNA-seq indicated regulated expression of this operon. High numbers of reads were found for TU7058 under most of the tested growth conditions, but relatively lower numbers were recorded after the cultures were transferred to high light (470 μmol photons m^{-2} s^{-1} for 30 min), and no reads were detected if the cultures were incubated in the dark for 12 h.[37]

The respective repeat spacer array is transcribed on the forward strand, starting from a single TSS approximately 6 kb away from the *cas* gene operon (Figure 1A). To explore the possible differential accumulation of leader and CRISPR RNAs (crRNAs), total RNA samples obtained from cultures grown under the same ten conditions as those previously used for differential RNA-seq were analyzed via northern hybridization. We used two probes complementary to the CRISPR leader RNA and the first two spacers and repeats, or spacers 1–4. The first probe produced a major signal of approximately 150 nt (Figure 1B, left), which matched the length of the leader (125 nt[25]) plus the length of the cleavage site within the first repeat (27 nt[19]), and two weaker signals matching the lengths of a repeat-spacer unit of ~72 nt and the final processed spacer 1 of 44 nt. The second probe detected the same ~150-nt precursor transcript due to overlap in the repeat but showed the strongest signals for repeat spacer units 2 and 3, which are somewhat longer (~75–77 nt) than other units. Their accumulation was highly dependent on the conditions. The strongest signals were obtained with samples from cultures exposed to cold stress, stationary phase, N, and C starvation, whereas the signals were weaker in samples from cultures exposed to heat shock or high light and were not detected in samples from cultures incubated in the dark for 12 h (Figure 1B, right). These results were consistent with the differential transcript accumulation observed for the CRISPR2 *cas10* operon by differential RNA-seq.[37]

Transcriptional regulation of the CRISPR2 *cas10* promoter

The observed differential accumulation of *cas* gene operon-mRNAs and crRNAs may be due to differential transcription, post-transcriptional regulation, or both. The prediction of a putative HLR1 motif in the CRISPR2 *cas10* (operon) promoter indicated possible transcriptional regulation. This HLR1 motif is

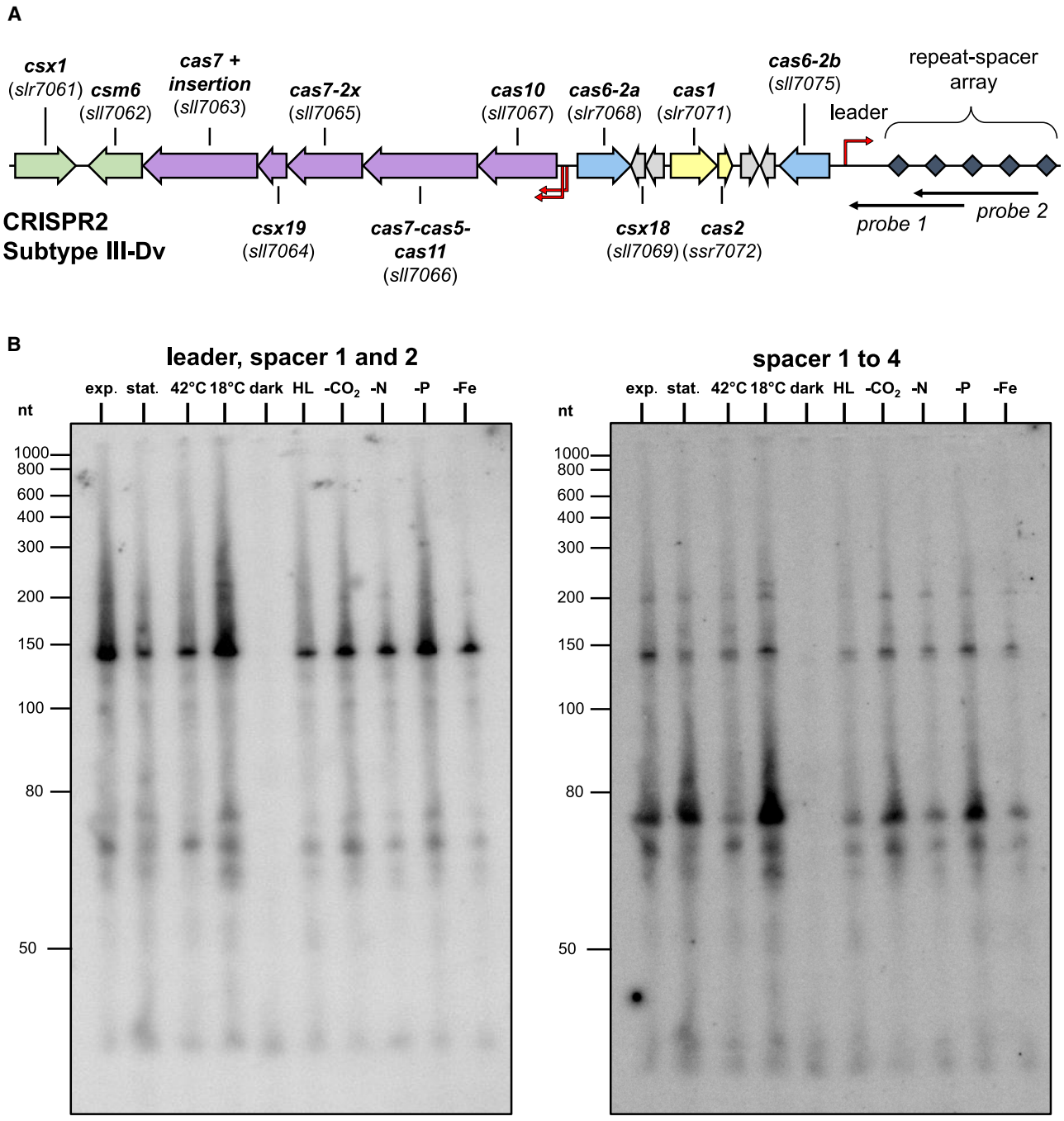

Figure 1. Organization of the type III-Dv (CRISPR2) locus in *Synechocystis* 6803 and the influence of environmental conditions

(A) The type III-Dv CRISPR-Cas system is located on the pSYSA plasmid. Several *cas* genes are located upstream of the CRISPR array, which consists of a 125-nt long leader and 56 spacers 34–46 nt in length interspaced by 37-nt long repeats (gray squares). Arrows in yellow indicate *cas* genes encoding proteins for the adaptation module; blue, *cas6* genes; purple, genes encoding the effector complex. Accessory genes are indicated by green arrows, and genes encoding hypothetical proteins are shown in light gray. The transcriptional start sites of the CRISPR array and effector complex operon are marked by bent red arrows, and the locations of the antisense RNA probes used for northern hybridization are indicated by straight narrow arrows in black.

(B) Influence of different environmental conditions on the accumulation of leader and crRNAs, including spacers 1 and 2 (left) and spacers 1–4 (right). For northern hybridization, ^{32}P-labeled transcript probes, as indicated in (A), were used after separation of 12 μg of RNA each isolated from cultures grown under 10 different conditions on a 10% urea-polyacrylamide gel. Exp. (exponential phase), stat. (stationary phase), 42°C (heat stress), 18°C (cold stress), dark (darkness), HL, high light (470 μmol photons m^{-2} s^{-1} for 30 min), -CO_2 (limitation in inorganic carbon supply), -N (nitrogen limitation), -P (phosphorus limitation), and -Fe (iron limitation). The membrane and 5S rRNA hybridization to control equal loading are shown in Figure 2A of our previous publication (Shan et al.).[38]

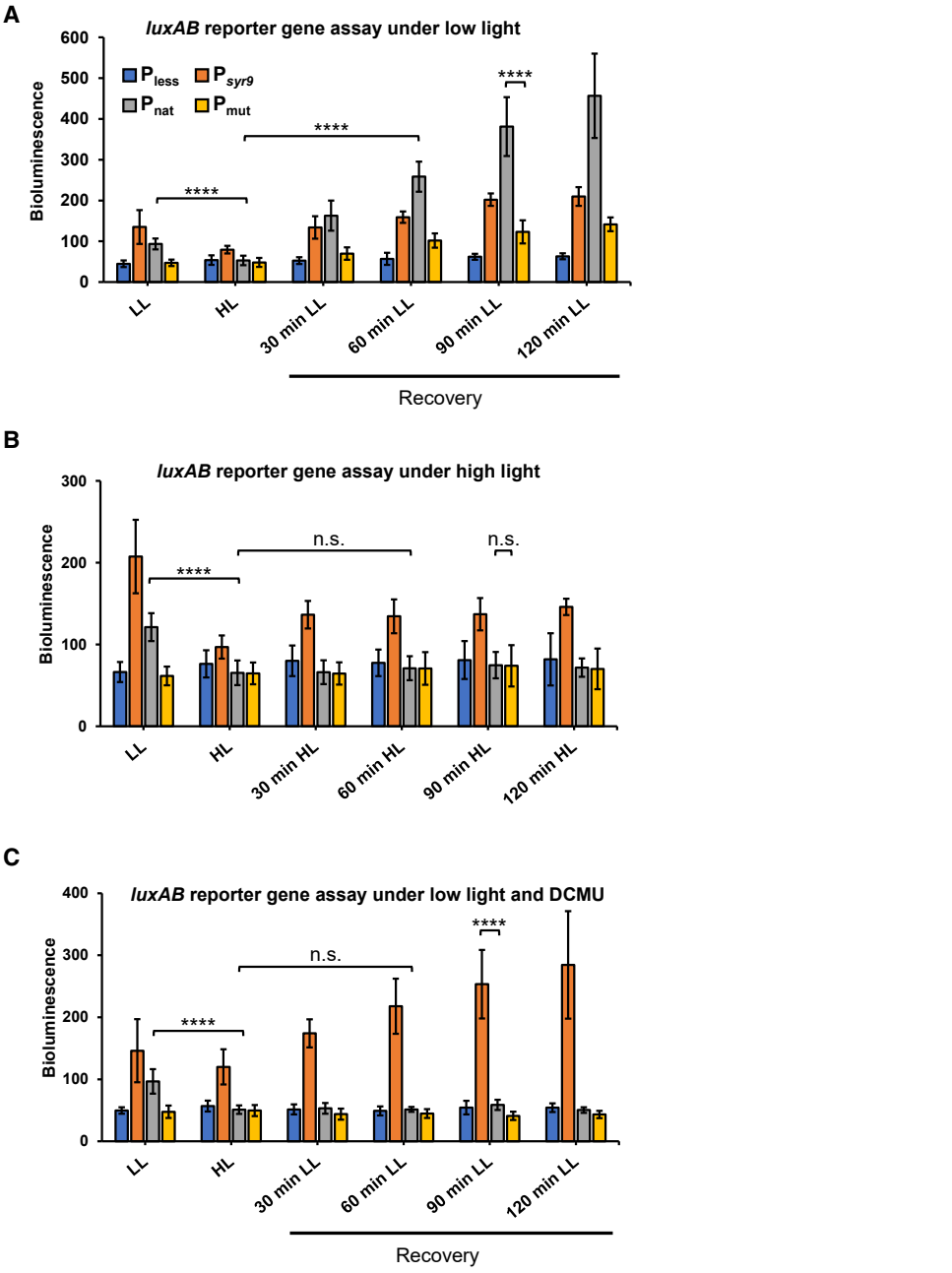

(legend on next page)

located −70 to −53 nt from the TSS of TU7063 and −172 to −155 nt from the TSS of TU7058. To examine its possible relevance, we cloned the 5′ UTR of the CRISPR2 *cas10* gene and the promoter region (+122 to −203 with regard to the TSS of TU7058), which included the HLR1 motif (native promoter [P_{nat}]) upstream of the *luxAB* reporter gene in the vector pILA.[39] As a control, we mutated the HLR1 motif by substituting four nucleotides with guanosines (mutated promoter [P_{mut}]). Initial P_{nat} activity was measured under low-light conditions. Promoter activity was measured again after a 4-h incubation under high light, where we observed a decrease in activity to the level of the no-promoter control (P_{less}). After transfer back to low light, P_{nat} activity increased significantly over time, reaching an approximately 10-fold increase in luminescence after 120 min (Figure 2A). In contrast, the P_{mut} promoter harboring the mutated HLR1 motif exhibited a basal level of bioluminescence, similar to that of the control strain harboring promoterless (P_{less}) *luxAB* genes, even after the P_{mut} strain was transferred back to low light. This finding indicates the importance of mutated nucleotides in the recognition and binding of RpaB to the promoter. When we exposed the cells after the initial 4 h continuously to high light (Figure 2B) or added the photosynthesis inhibitor 3-(3,4-dichlorophenyl)-1,1-dimethylurea (DCMU) (Figure 2C), bioluminescence remained at a basal level with P_{nat}, P_{mut}, and P_{less} for the duration of the experiment. This effect might be specifically related to RpaB and a change in redox status, as the P_{syr9} promoter used for control had modest activity under high-light conditions and was not negatively influenced by the added DCMU.

These results showed that the CRISPR2 *cas10* promoter is regulated by a redox-dependent mechanism involving the HLR1 motif. Furthermore, these results are consistent with the prediction that RpaB positively regulates this promoter, because it is known to dissociate from its HLR1 binding motif under high light.[40]

RpaB binds to the native CRISPR2 *cas10* promoter but not to the mutated HLR1 site

RpaB from *Synechocystis* 6803, fused to a C-terminal 6×histidine tag, was expressed as a recombinant protein (Figure S1) and used in electrophoretic mobility shift assays to validate the prediction that it regulates the transcription of the CRISPR2 effector complex. Increasing amounts of purified RpaB were incubated with Cy3-labeled DNA probes harboring either the wild type or the mutated HLR1 motif (P_{nat} and P_{mut}). As a positive control, we used the *psbA2* promoter, P_{psbA2}, which was previously characterized and contains a functional HLR1 motif.[41]

For the P_{nat} and P_{psbA2} fragments, a band shift was observed with a minimum of 50 pmol recombinant 6×His-RpaB, equaling a molecular ratio of 1:100. In previous experiments, a stoichiometric ratio of approximately 1:300–1:600 was required to observe a shift.[30,40,42] The differences may be due to different labeling methods (Cy3 DNA labeling versus 3′ end labeling with digoxigenin-ddUTP by terminal transferase) or minor differences in the purification. Overall, these results are comparable. In all studies, relatively high amounts were required for characterizing RpaB using *in vitro* assays. *In vivo*, activation of RpaB and binding to the HLR1 site depends on the redox status,[43,44] which is related to the respective light conditions and the phosphorylation of RpaB by the NblS/Hik33 kinase system.[45–47] In the absence of the cognate signals in *E. coli*, the recombinant protein may have lower affinity and not bind its target DNA as efficiently as *in vivo*, and therefore a relatively high concentration was required.

For the P_{mut} fragment with four substituted bases within the HLR1 motif, even the highest amount of 6×His-RpaB added (250 pmol) was not sufficient to induce a band shift (Figure 2D). This result was consistent with previous studies showing that such a base substitution in the first repeat prevents RpaB from binding to the HLR1 site.[30,40] To explain how the quadruple G mutation disrupts DNA binding, we searched for structural homologs of RpaB using HHpred.[48] Among the three hits with a score higher than 97% was the response regulator KpdE. KpdE recognizes an imperfect repeat of six nucleotides separated by five nucleotides,[49] resembling the HLR1 motif recognized by RpaB. In case of KdpE, an asymmetric heterodomain interface stabilizes the response regulator-DNA complex.[49] For both RpaB and KdpE, the binding site is an AT-rich region. In the case of KpdE, single nucleotide substitutions still allow partial binding of the protein to its cognate DNA, whereas dinucleotide changes in the repeat region abolished the interaction.[49] The comparison of their superimposed DNA binding domains in contact with DNA suggested that the corresponding sequence of RpaB intervenes into the major groove of the double helix. The substitution of an adenine by a guanine replaces a hydrogen donor by a hydrogen acceptor at the same spatial position in the DNA. This would eliminate the interaction with the side chain of the amino acid opposite the base. As the KdpE analysis showed, the loss of one such bond may not be enough to abolish binding, but several substitutions weaken the interaction enough to prevent binding of the protein to the DNA completely.[49]

Taken together, our results strongly suggested that the redox-dependent transcription factor RpaB positively regulates the transcription of the CRISPR2 effector complex genes under

Figure 2. RpaB control of the CRISPR2 *cas10* promoter

(A) Activity of the CRISPR2 *cas10* promoter under continuous low light after exposure to high light.

(B) Activity of the CRISPR2 *cas10* promoter after the shift to high light.

(C) Activity of the CRISPR2 *cas10* promoter under continuous low light in the presence of DCMU after exposure to high light. In (A)–(C), *Synechocystis* strains were transformed with pILA constructs with a promoterless *luxAB* (P_{less}), the sRNA Syr9 promoter (P_{syr9}), the wild type (P_{nat}), and the modified *cas10* promoter mutated in its HLR1 site (P_{mut}). Data are presented as mean ± SD from three independent experiments performed in triplicate each. ****$p < 0.001$ or $p > 0.05$ n.s. (not significant) by two-tailed Student's t test. For details of the statistical analyses, see Data S1.

(D) Electrophoretic mobility shift assays were used to test the binding of purified His-RpaB (Figure S1) to CRISPR2 *cas10* promoter fragments containing the native (P_{nat}) or mutated HLR1 sequence (P_{mut}). The HLR1-containing *psbA2* promoter fragment (P_{psbA2}) was used as a positive control. Substituted bases in the P_{mut} fragment are highlighted in red. The arrows represent imperfect repeats at the HLR1 site. HL, high light; LL, low light.

low-light conditions by binding to the HLR1 site. This finding implied that the expression of the CRISPR2 complex is activated under low-light conditions by RpaB and deactivated under high-light conditions when RpaB binding is lost. We wondered what this would mean for the accumulation of crRNAs. Moreover, upon acclimation to high light, RpaB regains DNA-binding activity.[30] Therefore, we performed another experiment in which we extended the time at high light to 6 h, transferred the cells to nitrogen starvation conditions, added the inhibitors DCMU or 2,5-dibromo-3-methyl-6-isopropylbenzoquinone (DBMIB), and analyzed the accumulation of CRISPR2 leader and crRNAs. Northern hybridization against spacers 1–4 produced several bands ranging from approximately 250 nt (pre-crRNA) to 72 nt (Figure 3A), corresponding to a single-unit crRNA precursor.[25] At approximately 150 nt, we observed a double band corresponding to partially processed pre-crRNAs, as shown also in Figure 1B. Because the spacers differ in sequence and length, the intermediate cleavage products differ slightly in size. Contrary to the results in Figure 1B, we observed no decrease, but a slight increase in the accumulation of pre-crRNA after 6 h of exposure to high light, which indicated that the cells had acclimated to the new environmental conditions (Figure 3A). In nitrogen-depleted medium, we observed a decrease in pre-crRNA accumulation after 6 h, consistent with the findings in Figure 1B and previous transcriptome analysis results.[37] To test the impact of changes in redox conditions on pre-crRNA accumulation, we added the inhibitors DCMU or DBMIB to our cultures. Here, we observed a weaker accumulation of the lower double bands at 150 nt. Furthermore, in the presence of DBMIB, mature crRNAs (<80 nt) vanished almost completely, which was consistent with the overall decrease in spacer transcript accumulation in the presence of the inhibitors. To test whether spacer and leader accumulation differed, we hybridized the same membrane against the leader transcript (Figure 3B). The signal ran at approximately 150 nt, matching the combined length for the leader transcript and the first repeat up to the first Cas6 cleavage site.[25] Leader and spacer-repeat accumulation were similar under high light and nitrogen depletion (Figure 3A). The addition of DCMU greatly reduced the accumulation of the leader compared with the standard (low-light) conditions, and the addition of DBMIB resulted in the loss of the leader transcript signal. The observed effects of DCMU and DBMIB could be explained by a general inhibitory effect on RNA synthesis. To test this possibility, we hybridized a probe for *atpT* mRNA, which was previously found to be strongly induced by addition of DCMU or DBMIB.[50,51] Both inhibitors upregulated the accumulation of *atpT* mRNA, indicating that transcription was not inhibited globally (Figure 3C).

These results suggest that the stability of the CRISPR2 leader transcript is linked to the redox status of the plastoquinone pool.

The CRISPR2 array promoter is highly active

We observed decreased accumulation of spacer-repeat and leader transcripts when the cells were exposed to high light (470 μmol photons m^{-2} s^{-1}) for 30 min (Figure 1B). To determine whether the promoter itself might be regulated, we used a promoter activity assay as for the CRISPR2 *cas10* promoter. Figure 3D shows the *luxAB* reporter assay with the CRISPR2 array promoter. The measured bioluminescence was extremely high, reaching 18,000 units, the highest measured activity in a comparison of 5 different promoters (Figure S2).

Moreover, we did not observe a decrease in the bioluminescence signal after exposing the cultures to high light for 30 min, but rather a further increase. These results suggested that the CRISPR2 array promoter was not influenced by environmental light conditions, and that the observed changes in leader and crRNA transcript levels were caused by another mechanism.

The CRISPR2 leader RNA interacts with CrhR

Because we found no evidence that RpaB controls the crRNA promoter, we considered preliminary results that indicated the involvement of the DEAD-box RNA helicase CrhR as another possible factor. CrhR mediates light- and redox-dependent responses in *Synechocystis* 6803.[31] Recombinant His-tagged native CrhR or $CrhR_{K57A}$ with enhanced RNA binding due to the K57A substitution within the ATP-binding motif were expressed and purified via affinity chromatography (Figure S3).

The recombinant proteins were incubated with *Synechocystis* 6803 total RNA and subjected to co-immunoprecipitation (coIP). Three cDNA libraries were prepared from the bound RNA in biological duplicates and utilized for Illumina sequencing (Table S1). The reads were trimmed, filtered, and mapped using Bowtie2.[52] Using the PEAKachu peak caller,[53] 39 peaks were identified in the CrhR library (Figure 4A; Table S2), and 41 peaks in the $CrhR_{K57A}$ library (Figures 4B; Table S3), which met a $\log_2$FC ≥ 1 and adjusted p value ≤ 0.05. Of these, 24 peaks were shared between the two proteins, including the CRISPR2 leader RNA (Figures 4A and 4B). Both the RNA helicase CrhR and the $CrhR_{K57A}$ mutant strongly interacted with their own mRNAs, consistent with previous reports of its autoregulation.[54] In addition to the leader, several CRISPR2 crRNAs were also enriched in the CrhR coIP (Figure 4C; Table S2).

The most highly enriched transcripts for $CrhR_{K57A}$ were asRNAs to the genes *sll0169*, *slr2000*, and *slr1494*, which encode the DUF4101 and DnaJ domain-containing protein Sll0169, the S-layer homology domain-containing protein Slr2000, and an ABC transporter subunit, respectively (Table S3).

Because the CRISPR2 leader RNA was enriched in the coIPs with both proteins, electrophoretic mobility shift assays were performed to validate the interactions. CRISPR2 leader RNA was synthesized *in vitro*, labeled with Cy3, and used as an RNA substrate. Binding of 2 pmol Cy3-labeled transcripts to various amounts of purified recombinant His-tagged CrhR or $CrhR_{K57A}$ was performed in the presence of poly(dI-dC) as a competitor. The CRISPR2 leader was shifted upon addition of as little as 1 pmol of CrhR (Figure 4D). We concluded that the CRISPR2 leader transcript was strongly bound by both CrhR and $CrhR_{K57A}$.

Effect of the Δ*crhR* mutation and redox stress conditions on CRISPR2 leader and crRNA accumulation

Next, we compared the effects of environmental stress conditions on CRISPR2 leader and repeat-spacer accumulation in *Synechocystis* 6803 wild type and the Δ*crhR* mutant. Cells were cultivated under standard growth conditions (low light and 30°C) and exposed to either 20°C or high light, followed

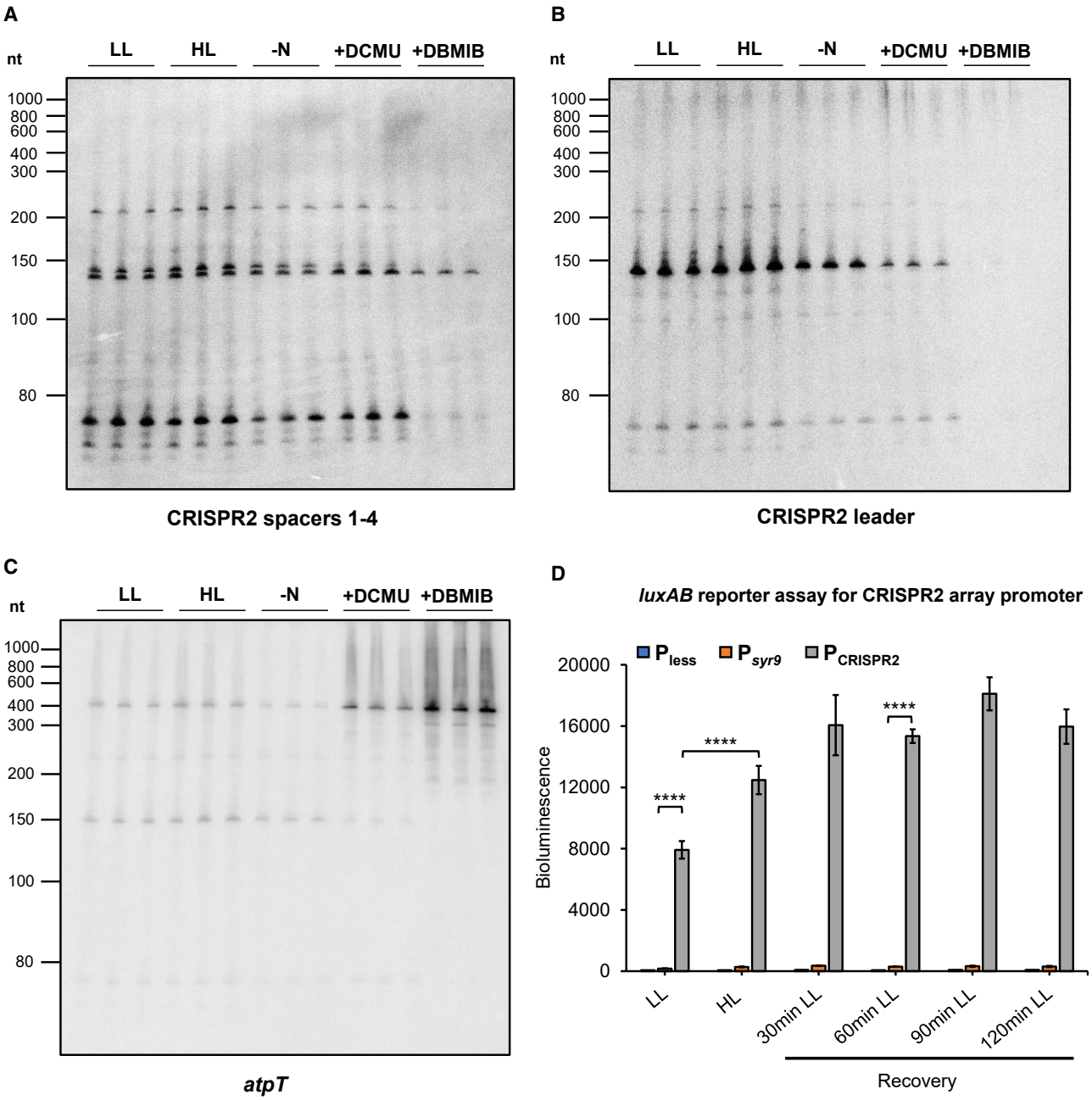

Figure 3. Effect of the addition of electron transport inhibitors on CRISPR leader accumulation

(A–C) *Synechocystis* 6803 wild type was cultivated under low light (LL), high light (HL), and nitrogen-depleted BG11 medium (-N) and in the presence of the inhibitors DCMU or DBMIB. Single-stranded RNA probes were hybridized against spacers 1–4 of CRISPR2 (A), CRISPR2 leader (B), and *atpT* mRNA (C). The relative amounts of CRISPR2 leader transcripts were normalized to the 5S rRNA intensity and quantified.

(D) Activity of the CRISPR2 array promoter under continuous low-light conditions or after exposure to high light. Data are presented as mean ± SD from three independent experiments performed in technical triplicates each. ****$p < 0.0001$, by two-tailed unpaired Student's t test. Details of the statistical analyses are presented in Data S1. A comparison of the activity of five different promoters is shown in Figure S2.

by recovery under low light. Total RNA was extracted and hybridized with probes against the CRISPR2 leader or spacers 1–4. When testing the wild type and mutant under standard and cold conditions (Figure 5A), we observed a lower level of CRISPR2 leader accumulation in Δ*crhR* than in the wild type. After normalizing signal intensities to 5S rRNA levels, we observed an approximately 40% signal reduction at 20°C in the wild type (Figure 5B). With respect to Δ*crhR*, we observed similar CRISPR2 leader transcript levels in both conditions, but generally lower levels than in the wild type. The accumulation of the

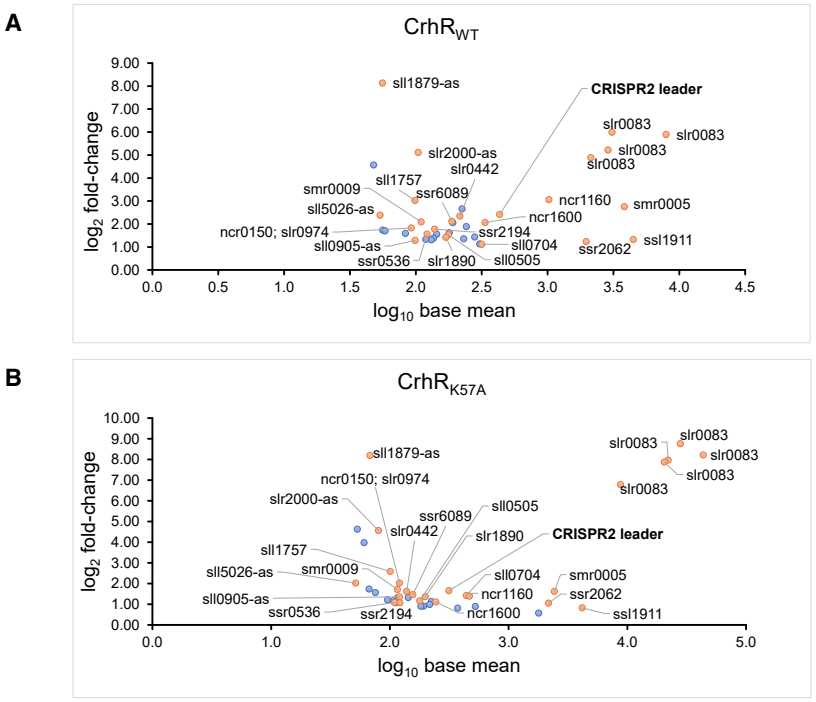

(legend on next page)

CRISPR2 leader transcript did not seem to be affected by temperature changes in Δ*crhR*. These results indicated that CrhR, on the one hand, had a basal stabilizing effect on CRISPR2 leader transcript accumulation, but that it had a destabilizing effect during temperature downshifts.

When testing the influence of high light on CRISPR2 leader and repeat spacer array transcript accumulation, we observed a rapid decrease in the accumulation of both transcripts after exposure to high light for 5 min (Figures 5C and 5D). The same observations were made after 30 min under high-light conditions. For recovery, the cultures were again exposed to low light, and cultivation continued for 2 h. After the recovery phase, the number of leader and repeat-spacer transcripts was similar to that before high-light exposure. These results suggest rapid degradation of the leader and spacer transcripts by an unknown mechanism and rapid adaptation to changes in the redox status of the cell.

Determination of CrhR amino acid residues interacting with the CRISPR2 leader

To confirm the interaction unambiguously and to identify the amino acid residues of CrhR that interact with the CRISPR2 leader, CrhR was crosslinked to CRISPR2 leader RNA *in vitro*. In total, we obtained 12 crosslinked peptide fragments for 2 replicates using UV and $CrhR_{K57A}$, 1 for CrhR and 3 for $CrhR_{K57A}$ using the chemical crosslinker 1,2,3,4-diepoxybutane (Figure 6A). The amino acid residues crosslinked to RNA were determined as described previously[55] and are shown in Figure 6B. None of the crosslinked amino acid residues were located within the known conserved motifs of DEAD-box RNA helicases (Figure S4). We used AlphaFold2[56,57] to predict the three-dimensional structure of CrhR. Consistent with recent reports that CrhR exists in solution predominantly as a homodimer,[58] AlphaFold modeled it as a dimer and predicted α helices and β folds in the most conserved part of the protein. No structure was predicted for the C-terminal section of the protein, which is consistent with the lack of sequence conservation (Figure 6C). The dimeric structure of these proteins is consistent with the homodimeric structure of the *Geobacillus stearothermophilus* RNA helicase CshA, the closest homolog of CrhR (43.57% sequence identity), for which the structure has been resolved.[59] The amino acid residues L103, F104, H225, C371, and P443 were located on the surface of CrhR, whereas C184 was not.

The importance of these six amino acids was then studied by generating different mutated CrhR variants and comparing their binding abilities by electrophoretic mobility shift assays. We introduced the amino acid substitutions L103G, F104G, H225A, C184A, C371A, and P443A. Cloning of a double ($CrhR_{H225\_C371A}$) and triple mutant ($CrhR_{L103G\_F104G\_H225A}$) was achieved through several rounds of site-directed mutagenesis. The cDNA of the hexamutant was ordered as gBlock (IDT) and cloned into the expression vector. Previously, structure prediction with AlphaFold2 indicated that the C-terminal domain (especially residues 375–427) is important for dimerization of CrhR.[58] Therefore, a fourth CrhR mutant was created with a shortened protein sequence (1–380) and lacking the C-terminal domain ($CrhR_{\Delta CTD}$). Electrophoretic mobility shift assays were performed with the four mutant and wild-type helicase ($CrhR_{WT}$). Different enzyme amounts were tested in conjunction with 2 pmol of *in vitro* transcribed CRISPR2 leader RNA as substrate. As a negative control, we tested an RNA of identical length, similar GC content, and minimum free energy. Results are shown in Figure S5.

For $CrhR_{WT}$, a shift was observed with the lowest amount tested (1 pmol) (Figure S5A). The shift intensity increased with the amount of $CrhR_{WT}$. An unspecific shift was observed with higher CrhR amounts (10–50 pmol). Interestingly, the triple mutant ($CrhR_{L103G\_F104G\_H225A}$) showed results similar to those observed for $CrhR_{WT}$, with a shift at the lowest protein amount tested (Figure S5B). This indicates that the RNA interactions by these residues were likely redundant. In contrast to the triple mutant, the double mutant required an increased helicase amount of 5 pmol to achieve a shift in substrate migration (Figure S5C). This result suggested that H225 and C371 were more important for RNA interaction than H225, L103, and F104. Residue C371 seemed to be of special importance as it is the only residue identified in the wild-type protein and the K57A mutant in the crosslinking experiment and also with both crosslinking methods (Figure 6A). The CrhR mutant carrying six substitutions showed the lowest affinity for the leader substrate and only at the highest protein concentration an unspecific shift was observed. This result corroborates the results of the crosslinking experiment, which indicated that these six residues were in contact with RNA (Figure S5D). Finally, truncated CrhR ($CrhR_{\Delta CTD}$), which likely cannot form a dimer, exhibited a shift, but only for the highest tested protein concentrations (Figure S5). This result suggests that CrhR is incapable of binding RNA effectively as a monomer and that a dimeric structure is necessary for high affinity. At higher concentrations, the control RNA was also bound by some of the CrhR variants suggesting a quite relaxed substrate recognition.

Figure 4. RNA target enrichment in the *in vitro* RNA pull-down from *Synechocystis* 6803 and specific interaction with the CRISPR2 leader

(A) Recombinant His-tagged CrhR was used.

(B) The $CrhR_{K57A}$ RNA helicase mutant was used. The peaks identified with PEAKachu[53] are shown in the MA plot. Based on two biological replicates, 39 CrhR and 41 $CrhR_{K57A}$ peaks were significantly enriched ($p_{adj} < 0.05$, $\log_2 FC > 0$). Common peaks for CrhR and $CrhR_{K57A}$ are orange colored, and the unique peaks are shown in blue.

(C) Enrichment of the CRISPR2 leader in the *in vitro* RNA pull-down from *Synechocystis* 6803 using recombinant His-tagged CrhR and $CrhR_{K57A}$. Colored plots show read coverage of the enriched RNAs. The experiment was performed in two biological replicates. CRISPR2 repeats and identified peaks are represented by magenta and blue boxes, respectively.

(D) Electrophoretic mobility shift assays showing the binding 1–50 pmol of CrhR (upper panel) and $CrhR_{K57A}$ (lower panel) to the CRISPR2 leader RNA. Representative results from two independent experiments are shown. For details of the expression and purification of recombinant CrhR-6×His and CrhRK57A-6×His see Figure S3.

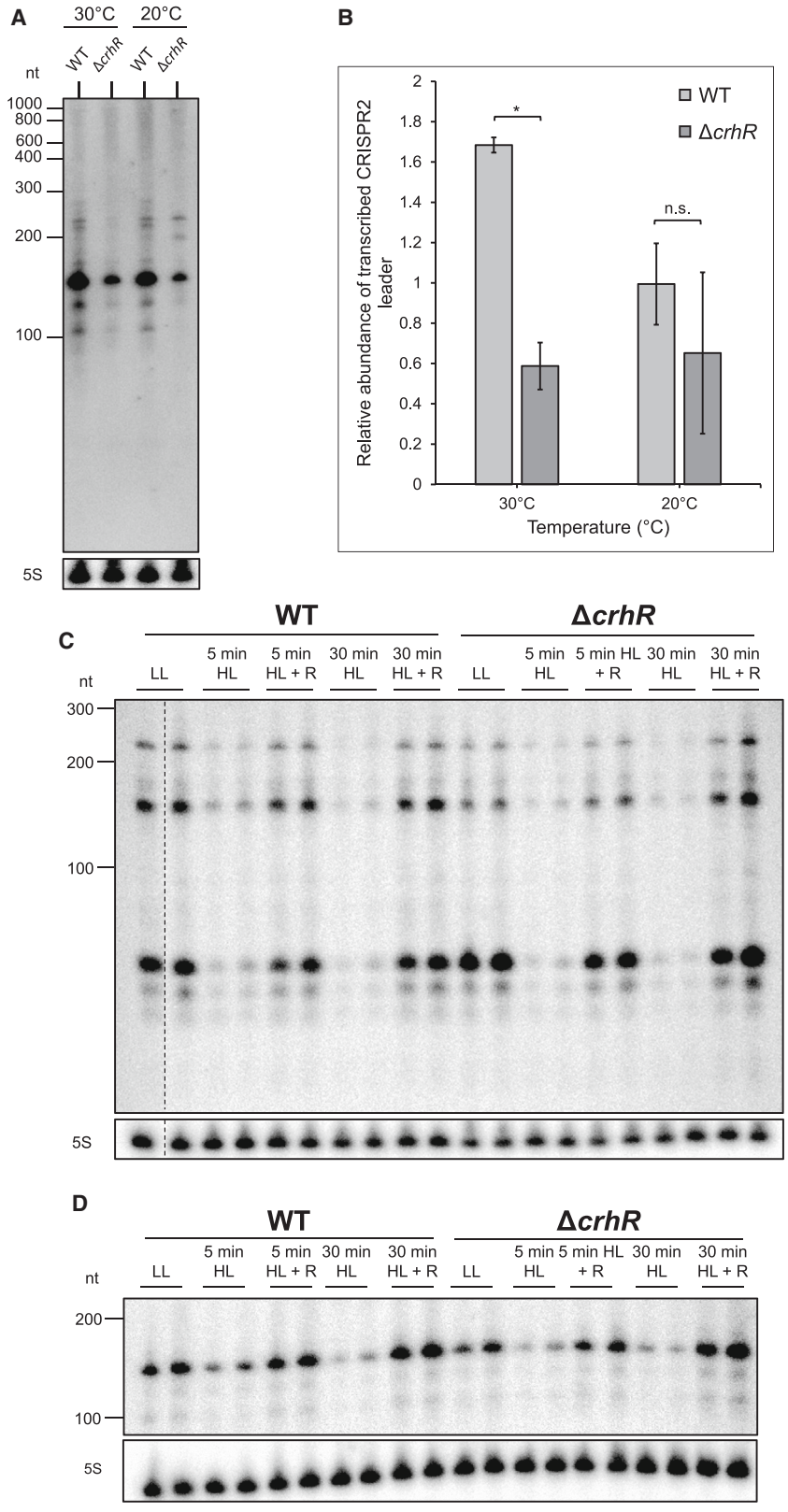

Figure 5. CRISPR2 leader and repeat-spacer accumulation in *Synechocystis* 6803 wild type and Δ*crhR* under cold and light stress conditions

(A) Impact of *crhR* deletion on CRISPR2 leader transcript accumulation. The wild type and Δ*crhR* were cultivated at 30°C or incubated at 20°C for 2 h. The strains were tested for accumulation of the CRISPR2 leader transcript by hybridization using a transcript probe. Hybridization of 5S rRNA is shown as the control for equal loading. A representative of biological duplicates is shown.

(B) Relative amounts of CRISPR2 leader transcripts were normalized to 5S rRNA intensity and quantified. Data are presented as mean ± SD from two independent experiments. *$p < 0.05$ and $p > 0.05$ n.s. (not significant) by two-tailed unpaired Student's t test. For details of the statistical analyses, see Data S1.

(C) Ten μg of total RNA from *Synechocystis* wild type and Δ*crhR* cultivated under low light (LL) or after exposure to high light (HL) for 5 or 10 min, with or without recovery for 2 h (R), was separated on a 10% denaturing polyacrylamide gel and hybridized with a ^{32}P-labeled transcript probe specific to spacer 1 to spacer 4.

(D) The same samples as in (C) but hybridized with a probe to the CRISPR2 leader. Hybridization of 5S rRNA was used as control of equal loading.

A

sample	XL_position	Position	XL_method	RNA_adduct
mt_DEB_Rep1	QQIEVCTIPNR	C371	DEB	U+C4H6O2
mt_DEB_Rep2	QQIEVCTIPNR	C371	DEB	G+C4H6O2
mt_DEB_Rep2	QQIEVCTIPNR	C371	DEB	U+C4H6O2
mt_UV_Rep1	QTACFSATM(Oxidation)PR	C184	UV	U
mt_UV_Rep1	IEQQLYHVPR	H225	UV	CU
mt_UV_Rep1	IEQQLYHVPR	H225	UV	U
mt_UV_Rep1	QQIEVCTIPNR	C371	UV	U
mt_UV_Rep1	SDWEVPEVDFNKPVLR	P443	UV	U
mt_UV_Rep1	LFILNVYGGQSIER	L103, F104	UV	U
mt_UV_Rep2	IEQQLYHVPR	H225	UV	U
mt_UV_Rep2	QQIEVCTIPNR	C371	UV	U
mt_UV_Rep2	IEQQLYHVPR	H225	UV	UU
mt_UV_Rep2	SDWEVPEVDFNKPVLR	P443	UV	U
mt_UV_Rep2	LFILNVYGGQSIER	L103, F104	UV	U
mt_UV_Rep2	LFILNVYGGQSIER	L103, F104	UV	UU
wt_UV_Rep2	QQIEVCTIPNR	C371	UV	U-H2O1-H1O3P1

B

MTNTLTSTFADLGLSEKRCQLLADIGFEAPTQIQTE
AIPLLLSGRDMLAQSQTGTGKTAAFALPLMDRIDPE
GDLQALILTPTRELAQQVAEAMKDFSHERR**LFILNV**
YGGQSIERQIRSLERGVQIVVGTPGRVIDLIDRKKL
KLETIQWVVLDEADEMLSMGFIDDVKTILRKTPPTR
QTACFSATMPREIKELVNQFLNDPALVTVKQTQSTP
TR**IEQQLYHVPR**GWSKAKALQPILEMEDPESAIIFV
RTKQTAADLTSRLQEAGHSVDEYHGNLSQSQRERLV
HRFRDGKIKLVVATDIAARGLDVNNLSHVVNFDLPD
NAETYIHRIGRTGRAGKTGKAIALVEPIDRRLLRSI
ENRLK**QQIEVCTIPNR**SQVEAKRIEKLQEQLKEALT
GERMASFLPLVRELSDEYDAQAIAAAALQMIYDQSC
PHWMK**SDWEVPEVDFNKPVLR**RGRNAGGGQNKSGGG
YQGKPGKPRRSSGGRRPAYSDRQQ

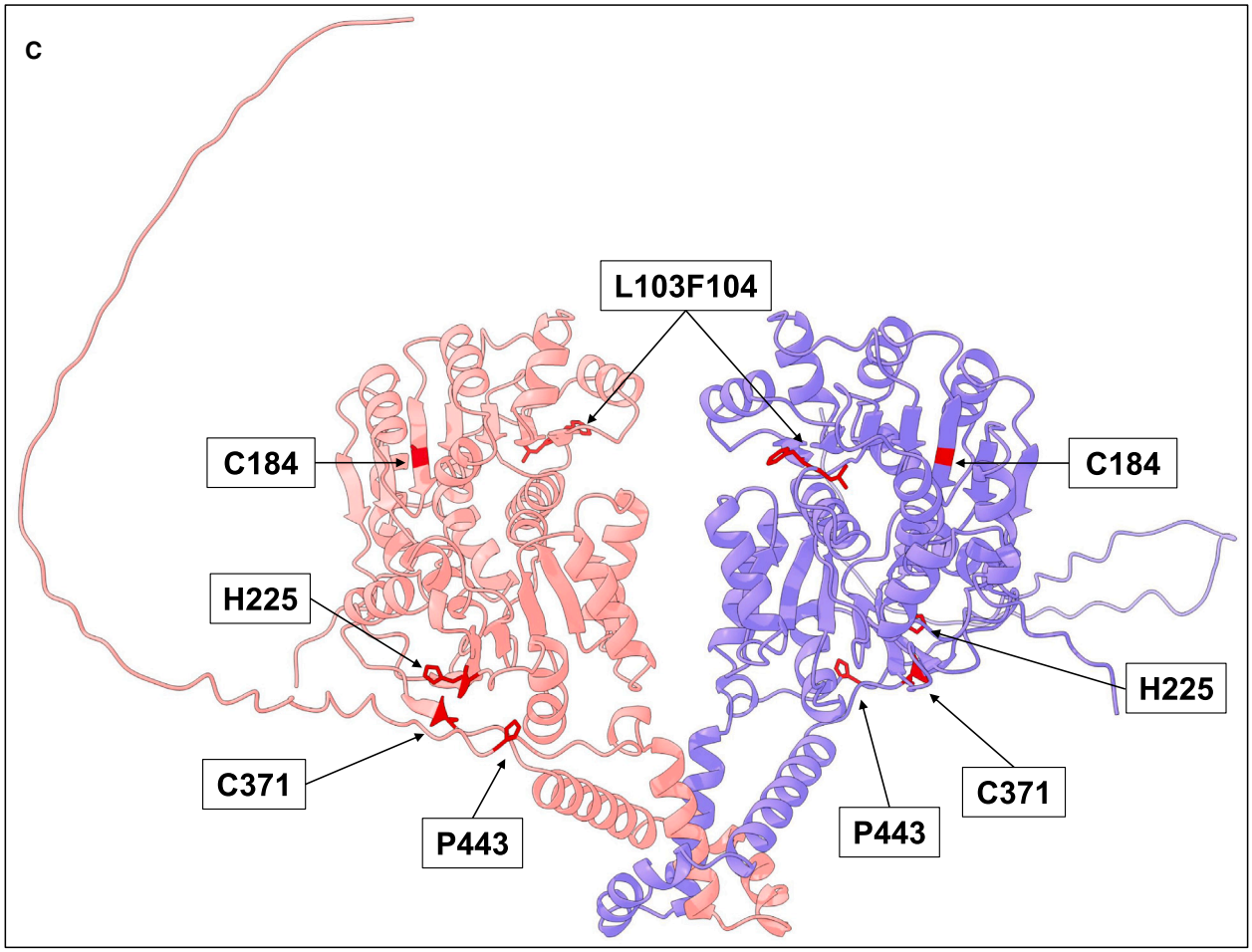

Figure 6. Crosslinking of CrhR to CRISPR2 leader RNA

(A) Overview of the peptide fragments and RNA adducts detected in two replicate samples harboring $CrhR_{K57A}$ (mt) or CrhR (wt). The crosslinked amino acid is highlighted in red and the numbered position is given.

(B) Sequence of CrhR. The amino acid residues of $CrhR_{K57A}$ crosslinked by UV treatment at 254 nm to the CRISPR2 leader are highlighted in red. The respective detected peptide fragments are underlined and in boldface letters. The QQIEVcTIPNR peptide was also detected for CrhR and in addition by chemical crosslinking using 1,2,3,4-diepoxybutane[60] (DEB) instead of UV treatment.

(C) Structure of a CrhR homodimer predicted by AlphaFold2[56,57] visualized in ChimeraX.[61] The CrhR amino acid residues crosslinked to the CRISPR2 leader transcript and identified by LC-MS are highlighted in red. The crosslinked CrhR residues in the context of conserved sequence segments and previously identified functionally relevant domains are given in Figure S4.

DISCUSSION

The main role of CRISPR-Cas systems is defense. Therefore, their constitutive expression might be expected. However, there is mounting evidence that some CRISPR-Cas systems, such as those in *E. coli*[7–10] and *S. islandicus*,[11,12] are regulated at the transcriptional level. When the risk of phage infection is high, CRISPR-Cas expression in *Pseudomonas aeruginosa* responds to environmental factors, such as temperature or high cell density; LasI/R and RhlI/R, two autoinducer pairs from the quorum sensing pathway, promote the expression of the type I-F CRISPR-Cas system.[15,16] Furthermore, resource availability can strongly influence *cas* gene expression. The cAMP receptor protein (CRP) binds to DNA in the presence of its co-factor cAMP, the level of which depends on the availability of glucose in the environment. In the phytopathogen *P. atrosepticum*, CRP increases the expression of type I-F *cas* genes when glucose is scarce,[14] whereas *cas* transcription is negatively regulated by the cAMP-CRP complex in the type I-E system of *E. coli* when glucose is available.[62]

Here, we show that RpaB, a DNA-binding response regulator, controls the transcription of the type III-Dv *cas* operon in the cyanobacterium *Synechocystis* 6803. RpaB is a redox-responsive transcription factor that is highly conserved in cyanobacteria and is a key regulator of light acclimation.[63] RpaB controls a large panel of genes relevant to photosynthesis, photoprotection, and membrane transport.[30] Analysis of the distribution of the HLR1 binding motif of RpaB in *Synechocystis* 6803 showed that RpaB functions as an activator under low-light conditions when the HLR1 motif is located at positions −66 to −45 to the TSS and as a repressor if located elsewhere in the promoter.[30] The finding that the abundance of crRNAs for the III-Dv system in *Synechocystis* 6803 varies greatly between different environmental conditions can therefore be partially explained by the control of the *cas* operon promoter by the binding of RpaB to HLR1 at an activating position. The availability of Cas proteins can limit the formation of Cas complexes and the protection of crRNAs bound to them. However, we were puzzled that the repeat-spacer array promoter, albeit very strong, not only lacked an HLR1 motif but also exhibited slightly greater activity in reporter gene assays under high light, contrary to the *cas* operon promoter.

This led us to consider the interaction between CrhR and the 125-nt leader transcript.[25] The CRISPR leader is usually understood as a longer region containing the promoter,[2,64] regulatory sequence elements important for adaptation,[65–67] and TSSs of the repeat-spacer array. CRISPR leaders have mostly been studied for their roles in spacer acquisition in the genome. However, they may also play an important role in the post-transcriptional regulation of pre-crRNAs and affect crRNA maturation and interference. The sRNA-dependent post-transcriptional regulation of a CRISPR array was identified in *P. aeruginosa*, where binding of the sRNA PhrS to the leader of a type I-F system repressed the Rho-dependent termination of CRISPR array transcription.[68]

We show that the CRISPR2 leader transcript also exists as a distinct sRNA in the cell and that its accumulation and that of crRNAs is strongly affected by the cellular redox status. We found that this leader RNA was highly enriched in *in vitro* coIPs with recombinant CrhR and $CrhR_{K57A}$. We confirmed the leader-CrhR (and leader-$CrhR_{K57A}$) interaction by electrophoretic mobility shift assays and identified the interacting amino acid residues by protein-RNA crosslinking coupled to mass spectrometry analysis.[55,69] The crosslinked residues L103/F104, H225, C371, C184, and P443 do not match positions previously described to be involved in the interactions between DEAD-box RNA helicases and their substrates.[70] However, these residues are in line with calculations of UV crosslinking efficiencies for different amino acids, which, among others, included phenylalanine (F), histidine (H), and proline (P), which were found here. Moreover, the systematic analysis of interactions between mutagenized RNA and protein variants suggested that π-stacking interactions between aromatic amino acids (such as Y, F, or H) and guanosine or uridine residues are important for crosslinking and for flanking amino acids,[71] whereas cysteine is prone to crosslinking due to its high reactivity.[69] Four of the six amino acids identified here matched these criteria, and L103 was flanked by aromatic amino acids on both sides (Figure S4). Moreover, with the exception of C184, these amino acids were predicted to be on the surface of the dimeric CrhR model (Figure 6C). Thus, both aspects are consistent with the possible involvement of these residues in RNA recognition and binding and indicate the potential for further analyses in the future.

RNA helicases are enzymes that can modify RNA structures. Therefore, they are associated with all aspects of RNA metabolism, such as the regulation of gene expression, RNA maturation and decay, transcription and packaging of RNA into ribonucleoprotein particles,[72,73] which are also relevant for the formation of CRISPR-Cas complexes. The expression of *crhR* is regulated by the redox status of the electron transport chain[31] and becomes strongly enhanced in response to a decrease in temperature.[74] CrhR plays a role in the modulation of multiple metabolic pathways during cold acclimation[35] and is indispensable for energy redistribution and the regulation of photosystem stoichiometry at low temperatures.[75] Consistent with these physiological functions, CrhR is localized to the thylakoid membrane, but also cosedimented with degradosome and polysome complexes.[76] Our data showed decreased leader and crRNA accumulation upon shifts to high light or low nitrogen, which was most pronounced upon addition of the inhibitor DBMIB, suggesting that these conditions constitute redox stress effects. A redox component involved in the expression of CRISPR-Cas systems has not yet been reported. However, such regulation is highly important for cyanobacteria, which are the only prokaryotes that perform oxygenic photosynthesis. In fact, phage adsorption to the cyanobacterial host, replication, modulation of host cell metabolism, and survival in the environment following lysis all exhibited light-dependent components.[77]

Indeed, the transcriptional control of *cas* gene transcription through RpaB and recruitment of the DEAD-box RNA helicase CrhR by the leader transcript are consistent with this mode of regulation (Figure 7). The involvement of CrhR in this process adds to recent reports on the connection between components of the degradosome and the type III CRISPR-Cas machinery.[21,78] Our results are furthermore consistent with recent results of unbiased screens that multiple host genes can affect CRISPR expression.[13] The here described parallel control of *cas* gene transcription by the transcription factor RpaB and the

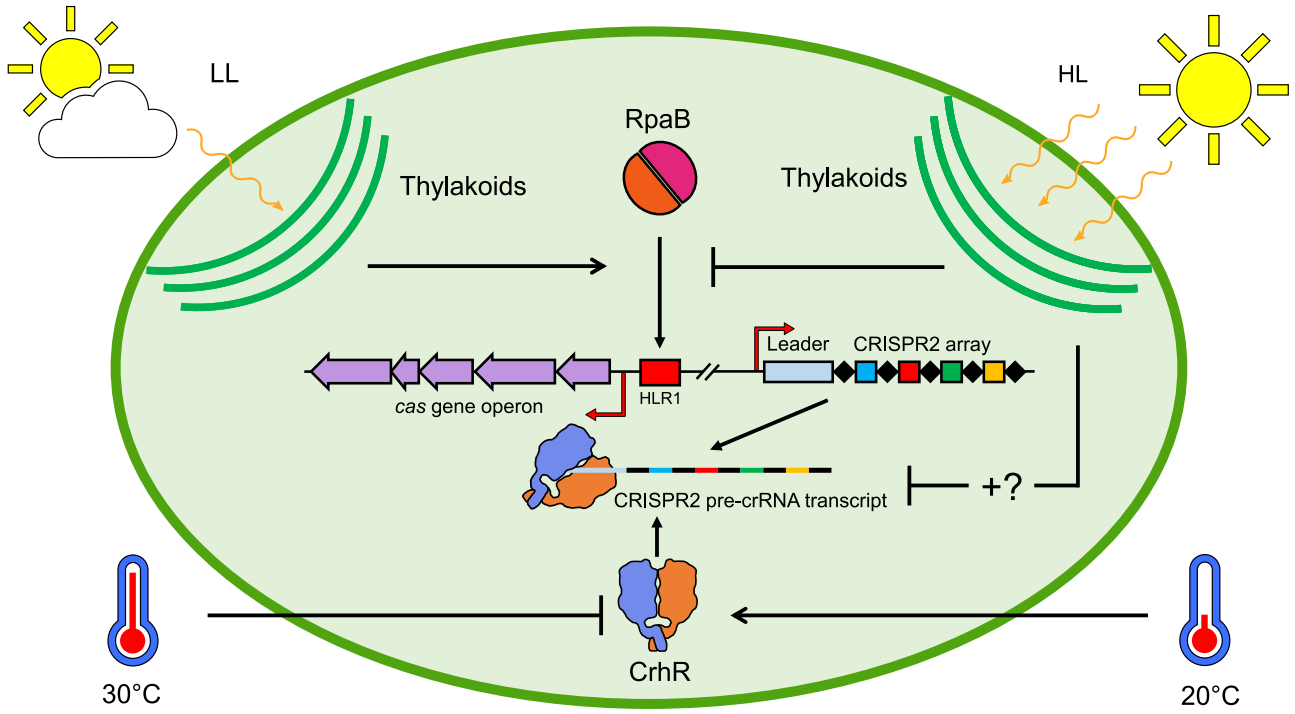

Figure 7. Multilevel redox control of CRISPR2 expression

The transcription factor RpaB binds to its HLR1 motif (red rectangle) under low light, initiating the expression of the *cas* operon (purple arrows), which encodes the effector complex of the type III-Dv system in *Synechocystis* 6803. Under high-light conditions, the change in the redox status of the photosystems, located in the thylakoid membrane (green arcs), causes RpaB to dissociate from its HLR1 motif, resulting in repression of the transcription of the *cas* gene operon. At the post-transcriptional level, high light leads to a decrease in the CRISPR2 leader and repeat-spacer transcript accumulation by an unknown mechanism (question mark). The DEAD-box RNA helicase CrhR recognizes the leader transcript at lower (20°C), but not at higher temperature (30°C). HL, high light; LL, low light.

effect of CrhR on CRISPR leader and crRNA accumulation highlights the intriguing complexity of CRISPR-Cas regulation in the context of the host cell.

Limitations of the study

Although the correlation between the cellular redox status and the activity of RpaB and CrhR is well established, many molecular details are missing on how the respective signals are transferred. The activation mechanism of CrhR is unknown. CrhR appears to have a wide range of substrate recognition; hence, it is a limitation that the exact recognition criteria are yet to be identified. The relatively high amounts of RpaB required in the electrophoretic mobility shift assays indicated that the recombinant protein was not as active as RpaB in the context of the cyanobacterial cell, where redox-dependent modifications by phosphorylation/dephosphorylation[45–47] and direct thiol modulation[43,44] occur.

STAR★METHODS

Detailed methods are provided in the online version of this paper and include the following:

- KEY RESOURCES TABLE
- RESOURCE AVAILABILITY
  - Lead contact
  - Materials availability
  - Data and code availability
- EXPERIMENTAL MODEL AND SUBJECTS DETAILS
  - Strains and growth conditions
- METHOD DETAILS
  - RNA isolation
  - Northern analysis
- CONSTRUCTION OF CRHR MUTANTS
  - Recombinant protein expression and purification
  - *In vitro* transcription of CRISPR2 leader
  - CrhR-CRISPR2 leader RNA cross-linking and enrichment of cross-linked peptide-RNA heteroconjugates
  - Analysis by mass spectrometry
  - Promoter activity assay
  - Electrophoretic mobility shift assay
  - *In vitro* his-tag affinity purification and RNA pulldown
  - Library preparation for RNA-seq
  - RNA-seq data analysis
- QUANTIFICATION AND STATISTICAL ANALYSIS

SUPPLEMENTAL INFORMATION

Supplemental information can be found online at https://doi.org/10.1016/j.celrep.2024.114485.

ACKNOWLEDGMENTS

This work was supported by the German Research Foundation priority program SPP2141 (grants HE 2544/14-2 to W.R.H. and UR225/7-2 to H.U.). We thank Yukako Hihara, Saitama, Japan, and Jogadhenu Prakash, Hyderabad, India, for the *E. coli* RpaB overexpression and *Synechocystis* Δ*crhR* strains, respectively. We thank Richard Reinhardt and his team, Cologne, Germany,

for sequence analyses. The support of Sergey Moshkovskiy and Olexandr Dybkov in interpreting the mass spectrometry data is greatly appreciated. We thank Viktoria Reimann, Freiburg, Germany, for cloning, purification, and testing of mutated CrhR variants, Monika Raabe, Göttingen and Ingeborg Scholz, Freiburg, Germany, for their expert technical assistance, and George Owttrim, Edmonton, Canada, for discussions about CrhR.

AUTHOR CONTRIBUTIONS

W.R.H. designed the work. Protein-RNA crosslinking experiments and identification of crosslinked peptide-RNA bonds were performed by A.W. and H.U. The analyses of RpaB effects, CRISPR2 leader, and repeat-spacer accumulation were performed by R.B. All the other CrhR-related experiments were carried out by A.M. The construction of cDNA libraries and the analysis of the pull-down results was performed by A.M. and C.S. A.M., R.B., and W.R.H. wrote the paper with contributions from all the authors.

DECLARATION OF INTERESTS

The authors declare no competing interests.

Received: December 20, 2023
Revised: May 26, 2024
Accepted: June 25, 2024
Published: July 10, 2024

REFERENCES

1. Makarova, K.S., Grishin, N.V., Shabalina, S.A., Wolf, Y.I., and Koonin, E.V. (2006). A putative RNA-interference-based immune system in prokaryotes: computational analysis of the predicted enzymatic machinery, functional analogies with eukaryotic RNAi, and hypothetical mechanisms of action. Biol. Direct *1*, 7. https://doi.org/10.1186/1745-6150-1-7.
2. Brouns, S.J.J., Jore, M.M., Lundgren, M., Westra, E.R., Slijkhuis, R.J.H., Snijders, A.P.L., Dickman, M.J., Makarova, K.S., Koonin, E.V., and van der Oost, J. (2008). Small CRISPR RNAs guide antiviral defense in prokaryotes. Science *321*, 960–964. https://doi.org/10.1126/science.1159689.
3. Makarova, K.S., Wolf, Y.I., Iranzo, J., Shmakov, S.A., Alkhnbashi, O.S., Brouns, S.J.J., Charpentier, E., Cheng, D., Haft, D.H., Horvath, P., et al. (2020). Evolutionary classification of CRISPR-Cas systems: a burst of class 2 and derived variants. Nat. Rev. Microbiol. *18*, 67–83. https://doi.org/10.1038/s41579-019-0299-x.
4. Makarova, K.S., Wolf, Y.I., Alkhnbashi, O.S., Costa, F., Shah, S.A., Saunders, S.J., Barrangou, R., Brouns, S.J.J., Charpentier, E., Haft, D.H., et al. (2015). An updated evolutionary classification of CRISPR-Cas systems. Nat. Rev. Microbiol. *13*, 722–736. https://doi.org/10.1038/nrmicro3569.
5. Özcan, A., Krajeski, R., Ioannidi, E., Lee, B., Gardner, A., Makarova, K.S., Koonin, E.V., Abudayyeh, O.O., and Gootenberg, J.S. (2021). Programmable RNA targeting with the single-protein CRISPR effector Cas7-11. Nature *597*, 720–725. https://doi.org/10.1038/s41586-021-03886-5.
6. van Beljouw, S.P.B., Haagsma, A.C., Rodríguez-Molina, A., van den Berg, D.F., Vink, J.N.A., and Brouns, S.J.J. (2021). The gRAMP CRISPR-Cas effector is an RNA endonuclease complexed with a caspase-like peptidase. Science *373*, 1349–1353. https://doi.org/10.1126/science.abk2718.
7. Pul, Ü., Wurm, R., Arslan, Z., Geissen, R., Hofmann, N., and Wagner, R. (2010). Identification and characterization of *E. coli* CRISPR-cas promoters and their silencing by H-NS. Mol. Microbiol. *75*, 1495–1512. https://doi.org/10.1111/j.1365-2958.2010.07073.x.
8. Westra, E.R., Pul, Ü., Heidrich, N., Jore, M.M., Lundgren, M., Stratmann, T., Wurm, R., Raine, A., Mescher, M., Van Heereveld, L., et al. (2010). H-NS-mediated repression of CRISPR-based immunity in *Escherichia coli* K12 can be relieved by the transcription activator LeuO. Mol. Microbiol. *77*, 1380–1393. https://doi.org/10.1111/j.1365-2958.2010.07315.x.
9. MacRitchie, D.M., Buelow, D.R., Price, N.L., and Raivio, T.L. (2008). Two-component signaling and gram negative envelope stress response systems. Adv. Exp. Med. Biol. *631*, 80–110. https://doi.org/10.1007/978-0-387-78885-2_6.
10. Perez-Rodriguez, R., Haitjema, C., Huang, Q., Nam, K.H., Bernardis, S., Ke, A., and DeLisa, M.P. (2011). Envelope stress is a trigger of CRISPR RNA-mediated DNA silencing in *Escherichia coli*. Mol. Microbiol. *79*, 584–599. https://doi.org/10.1111/j.1365-2958.2010.07482.x.
11. Liu, T., Liu, Z., Ye, Q., Pan, S., Wang, X., Li, Y., Peng, W., Liang, Y., She, Q., and Peng, N. (2017). Coupling transcriptional activation of CRISPR–Cas system and DNA repair genes by Csa3a in *Sulfolobus islandicus*. Nucleic Acids Res. *45*, 8978–8992. https://doi.org/10.1093/nar/gkx612.
12. He, F., Vestergaard, G., Peng, W., She, Q., and Peng, X. (2017). CRISPR-Cas type I-A Cascade complex couples viral infection surveillance to host transcriptional regulation in the dependence of Csa3b. Nucleic Acids Res. *45*, 1902–1913. https://doi.org/10.1093/nar/gkw1265.
13. Smith, L.M., Hampton, H.G., Yevstigneyeva, M.S., Mahler, M., Paquet, Z.S.M., and Fineran, P.C. (2024). CRISPR-Cas immunity is repressed by the LysR-type transcriptional regulator PigU. Nucleic Acids Res. *52*, 755–768. https://doi.org/10.1093/nar/gkad1165.
14. Patterson, A.G., Chang, J.T., Taylor, C., and Fineran, P.C. (2015). Regulation of the Type I-F CRISPR-Cas system by CRP-cAMP and GalM controls spacer acquisition and interference. Nucleic Acids Res. *43*, 6038–6048. https://doi.org/10.1093/nar/gkv517.
15. Høyland-Kroghsbo, N.M., Paczkowski, J., Mukherjee, S., Broniewski, J., Westra, E., Bondy-Denomy, J., and Bassler, B.L. (2017). Quorum sensing controls the *Pseudomonas aeruginosa* CRISPR-Cas adaptive immune system. Proc. Natl. Acad. Sci. USA *114*, 131–135. https://doi.org/10.1073/pnas.1617415113.
16. Høyland-Kroghsbo, N.M., Muñoz, K.A., and Bassler, B.L. (2018). Temperature, by controlling growth rate, regulates CRISPR-Cas activity in *Pseudomonas aeruginosa*. mBio *9*, e02184-18. https://doi.org/10.1128/mBio.02184-18.
17. Murray, A.G., and Eldridge, P.M. (1994). Marine viral ecology: incorporation of bacteriophage into the microbial planktonic food web paradigm. J. Plankton Res. *16*, 627–641. https://doi.org/10.1093/plankt/16.6.627.
18. Carlson, M.C.G., Ribalet, F., Maidanik, I., Durham, B.P., Hulata, Y., Ferrón, S., Weissenbach, J., Shamir, N., Goldin, S., Baran, N., et al. (2022). Viruses affect picocyanobacterial abundance and biogeography in the North Pacific Ocean. Nat. Microbiol. *7*, 570–580. https://doi.org/10.1038/s41564-022-01088-x.
19. Reimann, V., Alkhnbashi, O.S., Saunders, S.J., Scholz, I., Hein, S., Backofen, R., and Hess, W.R. (2017). Structural constraints and enzymatic promiscuity in the Cas6-dependent generation of crRNAs. Nucleic Acids Res. *45*, 915–925. https://doi.org/10.1093/nar/gkw786.
20. Kieper, S.N., Almendros, C., Behler, J., McKenzie, R.E., Nóbrega, F.L., Haagsma, A.C., Vink, J.N.A., Hess, W.R., and Brouns, S.J.J. (2018). Cas4 facilitates PAM-compatible spacer selection during CRISPR adaptation. Cell Rep. *22*, 3377–3384. https://doi.org/10.1016/j.celrep.2018.02.103.
21. Behler, J., Sharma, K., Reimann, V., Wilde, A., Urlaub, H., and Hess, W.R. (2018). The host-encoded RNase E endonuclease as the crRNA maturation enzyme in a CRISPR–Cas subtype III-Bv system. Nat. Microbiol. *3*, 367–377. https://doi.org/10.1038/s41564-017-0103-5.
22. Scholz, I., Lott, S.C., Behler, J., Gärtner, K., Hagemann, M., and Hess, W.R. (2019). Divergent methylation of CRISPR repeats and cas genes in a subtype I-D CRISPR-Cas-system. BMC Microbiol. *19*, 147–147.11. https://doi.org/10.1186/s12866-019-1526-3.
23. McBride, T.M., Schwartz, E.A., Kumar, A., Taylor, D.W., Fineran, P.C., and Fagerlund, R.D. (2020). Diverse CRISPR-Cas complexes require independent translation of small and large subunits from a single gene. Mol. Cell *80*, 971–979.e7. https://doi.org/10.1016/j.molcel.2020.11.003.
24. Schwartz, E.A., Bravo, J.P.K., Ahsan, M., Macias, L.A., McCafferty, C.L., Dangerfield, T.L., Walker, J.N., Brodbelt, J.S., Palermo, G., Fineran, P.C., et al. (2024). RNA targeting and cleavage by the type III-Dv CRISPR

effector complex. Nat. Commun. *15*, 3324. https://doi.org/10.1038/s41467-024-47506-y.

25. Scholz, I., Lange, S.J., Hein, S., Hess, W.R., and Backofen, R. (2013). CRISPR-Cas systems in the cyanobacterium *Synechocystis* sp. PCC6803 exhibit distinct processing pathways involving at least two Cas6 and a Cmr2 protein. PLoS One *8*, e56470. https://doi.org/10.1371/journal.pone.0056470.

26. Hein, S., Scholz, I., Voß, B., and Hess, W.R. (2013). Adaptation and modification of three CRISPR loci in two closely related cyanobacteria. RNA Biol. *10*, 852–864. https://doi.org/10.4161/rna.24160.

27. Makarova, K.S., Anantharaman, V., Grishin, N.V., Koonin, E.V., and Aravind, L. (2014). CARF and WYL domains: ligand-binding regulators of prokaryotic defense systems. Front. Genet. *5*, 102. https://doi.org/10.3389/fgene.2014.00102.

28. Garcia-Doval, C., Schwede, F., Berk, C., Rostøl, J.T., Niewoehner, O., Tejero, O., Hall, J., Marraffini, L.A., and Jinek, M. (2020). Activation and self-inactivation mechanisms of the cyclic oligoadenylate-dependent CRISPR ribonuclease Csm6. Nat. Commun. *11*, 1596. https://doi.org/10.1038/s41467-020-15334-5.

29. Ding, J., Schuergers, N., Baehre, H., and Wilde, A. (2022). Enzymatic properties of CARF-domain proteins in *Synechocystis* sp. PCC 6803. Front. Microbiol. *13*, 1046388. https://doi.org/10.3389/fmicb.2022.1046388.

30. Riediger, M., Kadowaki, T., Nagayama, R., Georg, J., Hihara, Y., and Hess, W.R. (2019). Biocomputational analyses and experimental validation identify the regulon controlled by the redox-responsive transcription factor RpaB. iScience *15*, 316–331. https://doi.org/10.1016/j.isci.2019.04.033.

31. Kujat, S.L., and Owttrim, G.W. (2000). Redox-regulated RNA helicase expression. Plant Physiol. *124*, 703–714. https://doi.org/10.1104/pp.124.2.703.

32. Chamot, D., Colvin, K.R., Kujat-Choy, S.L., and Owttrim, G.W. (2005). RNA structural rearrangement via unwinding and annealing by the cyanobacterial RNA helicase, CrhR. J. Biol. Chem. *280*, 2036–2044. https://doi.org/10.1074/jbc.M409700200.

33. Prakash, J.S.S., Krishna, P.S., Sirisha, K., Kanesaki, Y., Suzuki, I., Shivaji, S., and Murata, N. (2010). An RNA helicase, CrhR, regulates the low-temperature-inducible expression of heat-shock genes *groES, groEL1* and *groEL2* in *Synechocystis* sp. PCC 6803. Microbiology *156*, 442–451. https://doi.org/10.1099/mic.0.031823-0.

34. Georg, J., Rosana, A.R.R., Chamot, D., Migur, A., Hess, W.R., and Owttrim, G.W. (2019). Inactivation of the RNA helicase CrhR impacts a specific subset of the transcriptome in the cyanobacterium *Synechocystis* sp. PCC 6803. RNA Biol. *16*, 1205–1214. https://doi.org/10.1080/15476286.2019.1621622.

35. Rowland, J.G., Simon, W.J., Prakash, J.S.S., and Slabas, A.R. (2011). Proteomics reveals a role for the RNA helicase *crhR* in the modulation of multiple metabolic pathways during cold acclimation of *Synechocystis* sp. PCC6803. J. Proteome Res. *10*, 3674–3689. https://doi.org/10.1021/pr200299t.

36. Migur, A., Heyl, F., Fuss, J., Srikumar, A., Huettel, B., Steglich, C., Prakash, J.S.S., Reinhardt, R., Backofen, R., Owttrim, G.W., and Hess, W.R. (2021). The temperature-regulated DEAD-box RNA helicase CrhR interactome: Autoregulation and photosynthesis-related transcripts. J. Exp. Bot. *72*, erab416-7579. https://doi.org/10.1093/jxb/erab416.

37. Kopf, M., Klähn, S., Scholz, I., Matthiessen, J.K.F., Hess, W.R., and Voß, B. (2014). Comparative analysis of the primary transcriptome of *Synechocystis* sp. PCC 6803. DNA Res. *21*, 527–539. https://doi.org/10.1093/dnares/dsu018.

38. Zhan, J., Steglich, C., Scholz, I., Hess, W.R., and Kirilovsky, D. (2021). Inverse regulation of light harvesting and photoprotection is mediated by a 3'-end-derived sRNA in cyanobacteria. Plant Cell *33*, 358–380. https://doi.org/10.1093/plcell/koaa030.

39. Kunert, A., Hagemann, M., and Erdmann, N. (2000). Construction of promoter probe vectors for *Synechocystis* sp. PCC 6803 using the light-emitting reporter systems Gfp and LuxAB. J. Microbiol. Methods *41*, 185–194. https://doi.org/10.1016/s0167-7012(00)00162-7.

40. Kadowaki, T., Nagayama, R., Georg, J., Nishiyama, Y., Wilde, A., Hess, W.R., and Hihara, Y. (2016). A feed-forward loop consisting of the response regulator RpaB and the small RNA PsrR1 controls light acclimation of photosystem I gene expression in the cyanobacterium *Synechocystis* sp. PCC 6803. Plant Cell Physiol. *57*, 813–823. https://doi.org/10.1093/pcp/pcw028.

41. Eriksson, J., Salih, G.F., Ghebramedhin, H., and Jansson, C. (2000). Deletion mutagenesis of the 5′ *psbA2* region in *Synechocystis* 6803: Identification of a putative cis element involved in photoregulation. Mol. Cell Biol. Res. Commun. *3*, 292–298. https://doi.org/10.1006/mcbr.2000.0227.

42. Seino, Y., Takahashi, T., and Hihara, Y. (2009). The response regulator RpaB binds to the upstream element of photosystem I genes to work for positive regulation under low-light conditions in *Synechocystis* sp. strain PCC 6803. J. Bacteriol. *191*, 1581–1586. https://doi.org/10.1128/JB.01588-08.

43. Ibrahim, I.M., Rowden, S.J.L., Cramer, W.A., Howe, C.J., and Puthiyaveetil, S. (2022). Thiol redox switches regulate the oligomeric state of cyanobacterial Rre1, RpaA and RpaB response regulators. FEBS Lett. *596*, 1533–1543. https://doi.org/10.1002/1873-3468.14340.

44. Kato, N., Iwata, K., Kadowaki, T., Sonoike, K., and Hihara, Y. (2022). Dual redox regulation of the DNA-binding activity of the response regulator RpaB in the cyanobacterium *Synechocystis* sp. PCC 6803. Plant Cell Physiol. *63*, 1078–1090. https://doi.org/10.1093/pcp/pcac079.

45. Hsiao, H.-Y., He, Q., Van Waasbergen, L.G., and Grossman, A.R. (2004). Control of photosynthetic and high-light-responsive genes by the histidine kinase DspA: negative and positive regulation and interactions between signal transduction pathways. J. Bacteriol. *186*, 3882–3888. https://doi.org/10.1128/JB.186.12.3882-3888.2004.

46. Tu, C.-J., Shrager, J., Burnap, R.L., Postier, B.L., and Grossman, A.R. (2004). Consequences of a deletion in *dspA* on transcript accumulation in *Synechocystis* sp. strain PCC6803. J. Bacteriol. *186*, 3889–3902. https://doi.org/10.1128/JB.186.12.3889-3902.2004.

47. Yasuda, A., Inami, D., and Hanaoka, M. (2020). RpaB, an essential response regulator for high-light stress, is extensively involved in transcriptional regulation under light-intensity upshift conditions in *Synechococcus elongatus* PCC 7942. J. Gen. Appl. Microbiol. *66*, 73–79. https://doi.org/10.2323/jgam.2020.01.010.

48. Zimmermann, L., Stephens, A., Nam, S.-Z., Rau, D., Kübler, J., Lozajic, M., Gabler, F., Söding, J., Lupas, A.N., and Alva, V. (2018). A completely reimplemented MPI bioinformatics toolkit with a new HHpred server at its core. J. Mol. Biol. *430*, 2237–2243. https://doi.org/10.1016/j.jmb.2017.12.007.

49. Narayanan, A., Kumar, S., Evrard, A.N., Paul, L.N., and Yernool, D.A. (2014). An asymmetric heterodomain interface stabilizes a response regulator-DNA complex. Nat. Commun. *5*, 3282. https://doi.org/10.1038/ncomms4282.

50. Song, K., Baumgartner, D., Hagemann, M., Muro-Pastor, A.M., Maaß, S., Becher, D., and Hess, W.R. (2022). AtpΘ is an inhibitor of F0F1 ATP synthase to arrest ATP hydrolysis during low-energy conditions in cyanobacteria. Curr. Biol. *32*, 136–148.e5. https://doi.org/10.1016/j.cub.2021.10.051.

51. Song, K., Hagemann, M., Georg, J., Maaß, S., Becher, D., and Hess, W.R. (2022). Expression of the cyanobacterial FoF1 ATP synthase regulator AtpΘ depends on small DNA-binding proteins and differential mRNA stability. Microbiol. Spectr. *10*, e0256221. https://doi.org/10.1128/spectrum.02562-21.

52. Langmead, B., and Salzberg, S.L. (2012). Fast gapped-read alignment with Bowtie 2. Nat. Methods *9*, 357–359. https://doi.org/10.1038/nmeth.1923.

53. Bischler, T., Förstner, K.U., Maticzka, D., and Wright, P.R. (2021). PEAKachu: a peak calling tool for CLIP/RIP-seq data, Version v0.2.0 (Zenodo). https://doi.org/10.5281/zenodo.4669966.

54. Rosana, A.R.R., Whitford, D.S., Migur, A., Steglich, C., Kujat-Choy, S.L., Hess, W.R., and Owttrim, G.W. (2020). RNA helicase-regulated processing of the *Synechocystis rimO-crhR* operon results in differential cistron expression and accumulation of two sRNAs. J. Biol. Chem. *295*, 6372–6386. https://doi.org/10.1074/jbc.RA120.013148.

55. Sharma, K., Hrle, A., Kramer, K., Sachsenberg, T., Staals, R.H.J., Randau, L., Marchfelder, A., van der Oost, J., Kohlbacher, O., Conti, E., and Urlaub, H. (2015). Analysis of protein-RNA interactions in CRISPR proteins and effector complexes by UV-induced cross-linking and mass spectrometry. Methods *89*, 138–148. https://doi.org/10.1016/j.ymeth.2015.06.005.

56. Jumper, J., Evans, R., Pritzel, A., Green, T., Figurnov, M., Ronneberger, O., Tunyasuvunakool, K., Bates, R., Žídek, A., Potapenko, A., et al. (2021). Highly accurate protein structure prediction with AlphaFold. Nature *596*, 583–589. https://doi.org/10.1038/s41586-021-03819-2.

57. Mirdita, M., Schütze, K., Moriwaki, Y., Heo, L., Ovchinnikov, S., and Steinegger, M. (2022). ColabFold: making protein folding accessible to all. Nat. Methods *19*, 679–682. https://doi.org/10.1038/s41592-022-01488-1.

58. Whitman, B.T., Murray, C.R.A., Whitford, D.S., Paul, S.S., Fahlman, R.P., Glover, M.J.N., and Owttrim, G.W. (2022). Degron-mediated proteolysis of CrhR-like DEAD-box RNA helicases in cyanobacteria. J. Biol. Chem. *298*, 101925. https://doi.org/10.1016/j.jbc.2022.101925.

59. Huen, J., Lin, C.-L., Golzarroshan, B., Yi, W.-L., Yang, W.-Z., and Yuan, H.S. (2017). Structural Insights into a unique dimeric DEAD-box helicase CshA that promotes RNA decay. Structure *25*, 469–481. https://doi.org/10.1016/j.str.2017.01.012.

60. Bäumert, H.G., Sköld, S.-E., and Kurland, C.G. (1978). RNA-protein neighbourhoods of the ribosome obtained by crosslinking. Eur. J. Biochem. *89*, 353–359. https://doi.org/10.1111/j.1432-1033.1978.tb12536.x.

61. Pettersen, E.F., Goddard, T.D., Huang, C.C., Meng, E.C., Couch, G.S., Croll, T.I., Morris, J.H., and Ferrin, T.E. (2021). UCSF ChimeraX: Structure visualization for researchers, educators, and developers. Protein Sci. *30*, 70–82. https://doi.org/10.1002/pro.3943.

62. Yang, C.-D., Chen, Y.-H., Huang, H.-Y., Huang, H.-D., and Tseng, C.-P. (2014). CRP represses the CRISPR/Cas system in *Escherichia coli*: evidence that endogenous CRISPR spacers impede phage P1 replication. Mol. Microbiol. *92*, 1072–1091. https://doi.org/10.1111/mmi.12614.

63. Wilde, A., and Hihara, Y. (2016). Transcriptional and posttranscriptional regulation of cyanobacterial photosynthesis. Biochim. Biophys. Acta *1857*, 296–308. https://doi.org/10.1016/j.bbabio.2015.11.002.

64. Lillestøl, R.K., Shah, S.A., Brügger, K., Redder, P., Phan, H., Christiansen, J., and Garrett, R.A. (2009). CRISPR families of the crenarchaeal genus *Sulfolobus*: bidirectional transcription and dynamic properties. Mol. Microbiol. *72*, 259–272. https://doi.org/10.1111/j.1365-2958.2009.06641.x.

65. Erdmann, S., and Garrett, R.A. (2012). Selective and hyperactive uptake of foreign DNA by adaptive immune systems of an archaeon via two distinct mechanisms. Mol. Microbiol. *85*, 1044–1056. https://doi.org/10.1111/j.1365-2958.2012.08171.x.

66. Díez-Villaseñor, C., Guzmán, N.M., Almendros, C., García-Martínez, J., and Mojica, F.J.M. (2013). CRISPR-spacer integration reporter plasmids reveal distinct genuine acquisition specificities among CRISPR-Cas I-E variants of *Escherichia coli*. RNA Biol. *10*, 792–802. https://doi.org/10.4161/rna.24023.

67. Yosef, I., Shitrit, D., Goren, M.G., Burstein, D., Pupko, T., and Qimron, U. (2013). DNA motifs determining the efficiency of adaptation into the *Escherichia coli* CRISPR array. Proc. Natl. Acad. Sci. USA *110*, 14396–14401. https://doi.org/10.1073/pnas.1300108110.

68. Lin, P., Pu, Q., Wu, Q., Zhou, C., Wang, B., Schettler, J., Wang, Z., Qin, S., Gao, P., Li, R., et al. (2019). High-throughput screen reveals sRNAs regulating crRNA biogenesis by targeting CRISPR leader to repress Rho termination. Nat. Commun. *10*, 3728. https://doi.org/10.1038/s41467-019-11695-8.

69. Kramer, K., Sachsenberg, T., Beckmann, B.M., Qamar, S., Boon, K.-L., Hentze, M.W., Kohlbacher, O., and Urlaub, H. (2014). Photo-cross-linking and high-resolution mass spectrometry for assignment of RNA-binding sites in RNA-binding proteins. Nat. Methods *11*, 1064–1070. https://doi.org/10.1038/nmeth.3092.

70. Linder, P., and Jankowsky, E. (2011). From unwinding to clamping - the DEAD box RNA helicase family. Nat. Rev. Mol. Cell Biol. *12*, 505–516. https://doi.org/10.1038/nrm3154.

71. Knörlein, A., Sarnowski, C.P., de Vries, T., Stoltz, M., Götze, M., Aebersold, R., Allain, F.H.-T., Leitner, A., and Hall, J. (2022). Nucleotide-amino acid π-stacking interactions initiate photo cross-linking in RNA-protein complexes. Nat. Commun. *13*, 2719. https://doi.org/10.1038/s41467-022-30284-w.

72. Bourgeois, C.F., Mortreux, F., and Auboeuf, D. (2016). The multiple functions of RNA helicases as drivers and regulators of gene expression. Nat. Rev. Mol. Cell Biol. *17*, 426–438. https://doi.org/10.1038/nrm.2016.50.

73. Khemici, V., and Linder, P. (2018). RNA helicases in RNA decay. Biochem. Soc. Trans. *46*, 163–172. https://doi.org/10.1042/BST20170052.

74. Rosana, A.R.R., Chamot, D., and Owttrim, G.W. (2012). Autoregulation of RNA helicase expression in response to temperature stress in *Synechocystis* sp. PCC 6803. PLoS One *7*, e48683. https://doi.org/10.1371/journal.pone.0048683.

75. Sireesha, K., Radharani, B., Krishna, P.S., Sreedhar, N., Subramanyam, R., Mohanty, P., and Prakash, J.S.S. (2012). RNA helicase, CrhR is indispensable for the energy redistribution and the regulation of photosystem stoichiometry at low temperature in *Synechocystis* sp. Biochim. Biophys. Acta *1817*, 1525–1536. https://doi.org/10.1016/j.bbabio.2012.04.016.

76. Rosana, A.R.R., Whitford, D.S., Fahlman, R.P., and Owttrim, G.W. (2016). Cyanobacterial RNA helicase CrhR localizes to the thylakoid membrane region and cosediments with degradosome and polysome complexes in *Synechocystis* sp. strain PCC 6803. J. Bacteriol. *198*, 2089–2099. https://doi.org/10.1128/JB.00267-16.

77. Clokie, M.R.J., and Mann, N.H. (2006). Marine cyanophages and light. Environ. Microbiol. *8*, 2074–2082. https://doi.org/10.1111/j.1462-2920.2006.01171.x.

78. Chou-Zheng, L., and Hatoum-Aslan, A. (2019). A type III-A CRISPR-Cas system employs degradosome nucleases to ensure robust immunity. Elife *8*, e45393. https://doi.org/10.7554/eLife.45393.001.

79. Klähn, S., Baumgartner, D., Pfreundt, U., Voigt, K., Schön, V., Steglich, C., and Hess, W.R. (2014). Alkane biosynthesis genes in cyanobacteria and their transcriptional organization. Front. Bioeng. Biotechnol. *2*, 24. https://doi.org/10.3389/fbioe.2014.00024.

80. Rippka, R., Stanier, R.Y., Deruelles, J., Herdman, M., and Waterbury, J.B. (1979). Generic assignments, strain histories and properties of pure cultures of cyanobacteria. Microbiology *111*, 1–61. https://doi.org/10.1099/00221287-111-1-1.

81. Pinto, F.L., Thapper, A., Sontheim, W., and Lindblad, P. (2009). Analysis of current and alternative phenol based RNA extraction methodologies for cyanobacteria. BMC Mol. Biol. *10*, 79. https://doi.org/10.1186/1471-2199-10-79.

82. Kelly, C.L., Taylor, G.M., Hitchcock, A., Torres-Méndez, A., and Heap, J.T. (2018). A rhamnose-inducible system for precise and temporal control of gene expression in cyanobacteria. ACS Synth. Biol. *7*, 1056–1066. https://doi.org/10.1021/acssynbio.7b00435.

83. Beyer, H.M., Gonschorek, P., Samodelov, S.L., Meier, M., Weber, W., and Zurbriggen, M.D. (2015). AQUA cloning: a versatile and simple enzyme-free cloning approach. PLoS One *10*, e0137652. https://doi.org/10.1371/journal.pone.0137652.

84. Martin, M. (2011). Cutadapt removes adapter sequences from high-throughput sequencing reads. EMBnet. j. *17*, 10. https://doi.org/10.14806/ej.17.1.200.

STAR★METHODS

KEY RESOURCES TABLE

REAGENT or RESOURCE	SOURCE	IDENTIFIER
Bacterial and virus strains		
Synechocystis sp. PCC 6803	Cyanolab	Strain PCC-M
Synechocystis PCC 6803 luxCDE pILA-$P_{CRISPR2\_cas10nat}$	This work	N/A
Synechocystis PCC 6803 luxCDE pILA-$P_{CRISPR2\_cas10mut}$	This work	N/A
Synechocysts PCC 6803 pILA-P_{syrg}::luxAB	Klähn et al.[79]	N/A
Synechocystis PCC 6803_M Strain P*yfr2*:luxCDE	Klähn et al.[79]	N/A
Escherichia coli Rosetta (DE3) pLysS pET21a-RpaB-6×His	This work	N/A
Synechocystis 6803 Δ*crhR*	Migur et al.[36]; Prakash et al.[33]	N/A
Chemicals, peptides, and recombinant proteins		
[alpha-P32] UTP	Hartmann Analytic GmbH	Cat#SRP-210
[gamma-P32] ATP	Hartmann Analytic GmbH	Cat#SRP-301
Benzonase® Nuclease	Merck Millipore	Cat#70746-3
C18 (AQ 120 Å 5 μM)	Dr. Maisch GmbH	N/A
Coomassie Plus (Bradford) Assay Reagent	Thermo Fisher Scientific	Cat#23238
cOmplete™ EDTA-free Protease Inhibitor cocktail	Roche	Cat#04693132001
Cy3 Mono-Hydrazide	Cytiva	Cat#PA13120
Dynabeads™ His-Tag isolation and Pulldown	Invitrogen	Cat#10103D
LightShift™ poly(dIdC)	Thermo Fisher Scientific	Cat#20148E
Ni-NTA agarose Beads	Qiagen GmbH	Cat#30210
RNA 5′-polyphosphatase	Epicentre	Cat#RP8092H
Titansphere 5 μM	GL Science	N/A
T4 polynucleotide kinase	NEB	Cat#M0201S
tRNA for LightShift™	Thermo Fisher Scientific	Cat#20159
Turbo DNase	Thermo Fisher Scientific	Cat#AM2239
Critical commercial assays		
HiScribe® T7 Quick High Yield RNA Synthesis Kit	New England Biolabs	Cat# E2050S
MAXIscript™ T7 Transcription Kit	Invitrogen	Cat#AM1312
NucleoSpin® Gel and PCR Clean-up kit	Macherey-Nagel	Cat#740609.50
Q5® Site Directed Mutagenesis Kit	New England Biolabs	Cat#E0554S
RNA Clean and Concentrator-5	Zymo Research	Cat#R1013
ZR small-RNA PAGE Recovery Kit	Zymo Research	Cat# R1070
Deposited data		
Mass spectrometry datasets	Proteomics Identifications Database (PRIDE)	PRIDE: PXD047440
RNA-seq data	SRA database	SRA: SRX6451369 – SRX6451374
Oligonucleotides		
See Table S4		N/A
Recombinant DNA		
pET21a(+) -RpaB-6×His	Kadowaki et al.[40]	N/A
pQE70-crhR-6×His	Migur et al.[36]	N/A
pQE70-crhR(K57A)- 6×His	Migur et al.[36]	N/A
pILA-$P_{CRISPR2\_cas10nat}$	This work	N/A
pILA-$P_{CRISPR2\_cas10mut}$	This work	N/A
pet28a_CrhR_WT	This work	N/A

(*Continued on next page*)

Continued

REAGENT or RESOURCE	SOURCE	IDENTIFIER
pet28a_CrhR_ΔCTD	This work	N/A
pet28a_CrhR_H255_C371A	This work	N/A
pet28a_CrhR_L103G_F104G_H225A	This work	N/A
pet28a_CrhR L103G_F104G_C184A_ H225A_C371A__P443A	This work	N/A
Software and algorithms		
Alphafold2	Jumper et al.; Mirdita et al.[56,57]	https://colab.research.google.com/github/sokrypton/ColabFold/blob/main/AlphaFold2.ipynb
ChimeraX Version 1.4	Pettersen et al.[61]	https://www.cgl.ucsf.edu/chimerax/download.html
Quantity One	Bio-Rad	Version 4.6.6
Other		
Cryolis®	Bertin Technologies	N/A
Cultureplate™- 96	PerkinElmer	Cat#6005680
GeneQuant™ 100	GE Healthcare	N/A
HiTrap™Talon® crude 1 mL column	GE Healthcare (now Cytiva)	Cat#28-9537-66
Micro-organism lysing – VKMix 7 mL	Bertin Technologies	Cat#P000937-LYSK0-A
NanoDrop ND-1000 spectrophotometer	Peqlab	N/A
Precellys® 24-Dual	Bertin Technologies	N/A
Q Exactive HF instrument	Thermo Fisher Scientific	N/A
Supor-450 filters, 0.45 μm	Pall	Cat#61854
Supor®-800, 0.8 μm	Pall	Cat#65472
Typhoon™ FLA9500	GE Healthcare	N/A
UV Stratalinker™ 2400	Stratagene	N/A
Victor^3 1420 multilabel plate reader	PerkinElmer	N/A

RESOURCE AVAILABILITY

Lead contact

Further information and requests for resources and reagents should be directed to and will be fulfilled by the lead contact, Wolfgang R. Hess (wolfgang.hess@biologie.uni-freiburg.de).

Materials availability

All unique/stable reagents and strains generated in this study are available from the lead contact with a completed Material Transfer Agreement.

Data and code availability

- The RNA-seq data have been deposited in the SRA database https://www.ncbi.nlm.nih.gov/sra/and are openly available under the accession numbers SRX6451369–SRX6451374. All mass spectrometry proteomics datasets analyzed during this study are available in the Proteomics Identifications Database (PRIDE, at https://www.ebi.ac.uk/pride/) under the project accession number PXD047440.
- This paper does not report original code.
- Any additional information required to reanalyze the data reported in this work paper is available from the lead contact upon request.

EXPERIMENTAL MODEL AND SUBJECTS DETAILS

Strains and growth conditions

Cultures of the wild type and different mutant strains of *Synechocystis* 6803[33,36] were grown at 30°C in liquid BG11 medium[80] supplemented with 20 mM TES (N-[Tris-(hydroxymethyl)-methyl]-2-aminoethane sulfonic acid) under continuous illumination with white light at 30–50 μmol photons m^{-2} s^{-1} and continuous shaking.

Synechocystis 6803 strain Δ*crhR* was grown in BG11 in the presence of the appropriate antibiotics at the following concentrations: spectinomycin (sp) (20 μg/mL) and kanamycin (km) (50 μg/mL). For the cold and high light stress experiments, *Synechocystis* 6803 strains were cultivated until OD_{750nm} = 0.6 was reached. For cold stress, the cultures were then split into two groups: one was continued at 30°C, and the second was placed in a water bath at 20°C for 2 h. Under high-light conditions, if not otherwise indicated, the cells were exposed to 300 μmol m^{-2} s^{-1} for 5–30 min. For recovery, the cells were returned to low-light conditions (30–50 μmol photons m^{-2} s^{-1}) for 2 h.

For the experiment in Figure 3, *Synechocystis* 6803 was cultivated under low light (LL), high light (HL), in nitrogen-depleted BG11 media (-N) and in the presence of the inhibitors DCMU or DBMIB, 50 μM each. Cells were harvested after 6 h of incubation for RNA isolation.

E. coli strains were grown in liquid LB media (10 g L^{-1} bacto-tryptone, 5 g L^{-1} bacto-yeast extract, 10 g L^{-1} NaCl) with continuous agitation or on agar-solidified (1.5% [w/v] Bacto agar) LB supplemented with appropriate antibiotics at 37°C.

METHOD DETAILS

RNA isolation

Synechocystis 6803 cells were collected by vacuum filtration through hydrophilic polyethersulfone filters (Pall Supor-800, 0.8 μm), transferred to a tube containing 1 mL of PGTX buffer,[81] snap-frozen in liquid nitrogen and stored at −80°C until further use. RNA was extracted as described previously,[36] and the RNA concentration was determined using a NanoDrop ND-1000 spectrophotometer (Peqlab).

Northern analysis

RNA samples (10 μg) were denatured for 10 min at 70°C in loading buffer (Thermo Fischer Scientific, MA, USA), separated on 8 M urea −10% polyacrylamide gels for 16–18 h at 70 V and transferred to Amersham Hybond-N+ membrane (Cytiva, MA, USA) by electroblotting for 1 h at 1 mA cm^{-2}. The membranes were hybridized with specific [γ-^{32}P] ATP end-labelled oligonucleotides for 5S or [α-^{32}P] UTP-incorporated transcripts. Oligonucleotide and transcript probes were prepared using the T4-polynucleotide-kinase kit or the MAXIscript T7 Transcription (both from Thermo Fisher Scientific), respectively. Oligonucleotides used for the preparation of the probes are listed in Table S4 (32–39). Hybridization in 50% deionized formamide (≤ pH 7), 7% SDS, 250 mM NaCl and 120 mM $Na(PO_4)$ pH 7.2 was performed over night at 45°C or at 62°C with labeled oligonucleotide probes or labeled transcript probes, respectively. The membranes were washed in 2×SCC (3 M NaCl, 0.3 M sodium citrate, pH 7.0), 1% SDS for 10 min; 1×SCC, 0.5% SDS for 10 min and in 0.1×SCC, 0.1% SDS for up to 10 min. All wash steps were performed 5°C below hybridization temperature. Signals were detected with a Typhoon FLA9500 (Cytiva) and analyzed with Quantity One software (BIO-RAD).

CONSTRUCTION OF crhR MUTANTS

The *crhR* mutants were constructed using the Q5 Site-Directed Mutagenesis Kit (NEB). For pQE70_crhR_H255A, primers crhR_H225A_fw/rev and the plasmid pQE70_CrhR_WT were used. The PCR product was subcloned into Top10F' (Thermo Fisher Scientific). After sequencing, the isolated plasmid was used as a PCR template to introduce the C371A or L103G_F104G mutations (crhR_C371A_fw/rev or crhR_L103A_F104A_fw/rev, respectively). Primers crhR_delta_CTD_rev and pQE70_crhR-fw were used for reverse amplification of pQE70_CrhR_WT to generate a C-terminally truncated version of CrhR (amino acids 1–380), pQE70_crhR_ΔCTD. The PCR product was treated with FastDpnI (Thermo Fisher Scientific) and subcloned into Top10F'. To generate the 6-fold mutant CrhR_L103G_F104G_C184A_H225A_C371A_P443A, the gene was ordered as gBlocks (IDT) and amplified by PCR (PCRBio, Nippon Genetics) with primers pQE70_crhR_new_fw/rev. pQE70 was PCR amplified with primers pQE70 backbone for and pQE70_Gibson_Codonopt_rev and treated with FastDpnI. Both fragments were mixed and transformed into Top10F'. All plasmids isolated were sequenced (Microsynth). Due to frequently occurring mutations in the coding or promoter region, the pQE70 plasmid with the T5 promoter was replaced by the pet28a(+) plasmid carrying the T7 promoter. Therefore, primers pet28a+_fwd/rev were used for backbone amplification and primers CrhR_pet28_fwd and CrhR_pet28_rev (or CrhR_dCTD_pet28_rev for the truncated version) were used to amplify the WT and mutated CrhR versions from the respective sequenced pQE70 constructs. All fragments were treated with FastDpnI, mixed and subcloned into DH5α(NEB). The resulting plasmids were transformed into Rosetta(DE3)pLysS competent cells (Sigma).

Recombinant protein expression and purification

E. coli M15[pREP4] was transformed with the vectors pQE70:crhR-6×His and pQE70:crhR$_{K57A}$-6×His for overexpression of the recombinant His-tagged proteins CrhR and CrhR$_{K57A}$. Overnight cultures were diluted 1:100 in fresh LB medium supplemented with ampicillin and km and grown to an OD_{600} of 0.7. Protein expression was induced by adding isopropyl-β-D-thiogalactopyranoside (IPTG; 1 mM final concentration). Three hours after IPTG induction, the cells were harvested by centrifugation at 6,000 × g for 10 min at room temperature. The cell pellets were resuspended in lysis buffer (50 mM NaH_2PO_4 (pH 8), 1 M NaCl, 10% glycerol, 15 mM imidazole, and cOmplete Protease Inhibitor Cocktail (Roche)) and lysed using the One Shot Constant Cell Disruption System (Constant Systems Limited, United Kingdom) at 2.4 kbar. Cell debris was pelleted by centrifugation at 13,000 × g for 30 min at 4°C,

and the lysate was filtered through 0.45 μm Supor-450 filters (Pall). Recombinant proteins were immobilized on a HiTrap Talon crude 1 mL column (GE Healthcare), equilibrated with buffer A (50 mM NaH_2PO_4 (pH 8), 500 mM NaCl), and eluted with elution buffer B (50 mM NaH_2PO_4 (pH 8), 500 mM imidazole, 500 mM NaCl).

Recombinant His-tagged RpaB protein was expressed in Rosetta (DE3) + pLysS expression strain. The preculture (10 mL) was seeded into 1 L of phosphate-buffered TB medium. Expression of His-tagged RpaB was induced with 100 μM IPTG when cultures reached a density of 0.6–0.7 OD_{600nm}. After cultivating for 3 h at 37°C, cells were harvested by centrifugation (15 min at 4,000 × g), washed and resuspended in 20 mL of the lysis buffer (50 mM HEPES-KOH, pH 7.5, 150 mM NaCl, 10 mM $MgCl_2$ and 20 mM imidazole). All protein purification steps were performed at 4°C. Resuspended cells were transferred to VKMix_7 mL tubes (4 mL of resuspension per tube) and disrupted using Precellys 24 and Cryolis cooling system (Bertin Technologies) for three rounds with the following settings: 6000 rpm, 3 × 10 s and then centrifuged at 16,000×g for 20 min. The resulting supernatant was loaded onto 0.5 mL of Ni-NTA agarose beads (Qiagen GmbH), pre-equilibrated with lysis buffer, and incubated for 1 h with gently shaking to bind 6×His-tagged proteins. The column was washed twice with 2.5 mL wash buffer (lysis buffer containing 40 mM imidazole) and eluted with 0.5 mL of elution buffer (lysis buffer containing 300 mM imidazole). Eluates containing purified His-RpaB were desalted using a Vivaspin 20 10,000 MWCO and washed with desalting buffer (50 mM HEPES-KOH, pH 7.5, 10 mM $MgCl_2$). Protein concentration was determined by the Bradford assay. One microliter of protein sample was mixed with 200 μL Coomassie Plus Assay Reagent (Thermo Fisher Scientific) in a 96-well plate. The absorption at 595 nm was measured using a Victor[3] 1420 multilabel plate reader (PerkinElmer). Protein concentration was calculated using a bovine serum albumin calibration curve. After the addition of 20% (v/v) glycerol, the eluate was frozen in liquid N_2 and stored at - 80°C prior to use.

For Figure S5, all CrhR variants expressed from a pet28a(+) vector, were cultivated in 500 mL LB medium. After induction with 1 mM IPTG, cells were grown at 37°C for 3 h. Cells were harvested and pellets were stored at −20°C. Cell disruption (3 cycles of 3 × 6,500 rpm for 15 s with 10 s breaks in between) was performed using a Precellys 24 Dual homogenizer (Bertin) under nitrogen cooling. Filtered lysates were used for protein purification using an Äkta start system (GE Healthcare). Lysis buffer containing 50 mM NaH_2PO_4, 500 mM NaCl and 20 mM imidazole (pH 8) and wash buffer containing 40 mM imidazole were used. 1 mL HisTrap HP His-tag protein purification columns (Cytiva) were used. Elution was performed in a gradient from 40 to 500 mM imidazole. Fractions containing purified protein were pooled and protein concentrations were determined using the Direct Detect spectrometer (Merck), and purified proteins were stored at −80°C with 50% glycerol.

In vitro transcription of CRISPR2 leader

In vitro transcripts were prepared using the HiScribe T7 Quick High Yield RNA Synthesis Kit (NEB). For Figure S5, Templates were amplified by PCR using primers C2_leader_T7_fw/rev for CRISPR2 leader transcript and primers EMSA_CrhR_ctrl_T7_Fw/rev for the control transcript, otherwise, primers EMSA_CRISPR2LeadeR-T7_Fw/Rv were used to amplify the transcription template. Transcripts were size separated by denaturing 8 M urea 10% PAGE, visualized with ethidium bromide under ultraviolet (UV) light and excised at the appropriate size. The transcripts were purified using the ZR small-RNA PAGE Recovery Kit (Zymo Research).

CrhR-CRISPR2 leader RNA cross-linking and enrichment of cross-linked peptide-RNA heteroconjugates

We used 10 min of UV irradiation at 254 nm to covalently cross-link approximately 1 nmol of the complex formed between CRISPR2 leader RNA and the CrhR protein in a volume of 100 μL in buffer containing 50 mM NaH_2PO_4, 300 mM NaCl, and 250 mM imidazole (pH 8.0) as described previously.[21] Subsequently, cross-linked peptide–RNA heteroconjugates were enriched according to our previously established workflow.[55,69] We ethanol-precipitated the samples and resuspended the pellet in buffer containing 4 M urea and 50 mM Tris-HCl (pH 7.9). The urea concentration was subsequently decreased to 1 M by adding 5 vol of 50 mM Tris-HCl (pH 7.9). The RNA was hydrolyzed by adding 1 μg of RNase A and T1 (Ambion, Applied Biosystems) at 52°C for 2 h, followed by digestion with 25 U benzonase at 37°C for 1 h and trypsin (Promega) digestion overnight at the same temperature. To remove the non-cross-linked RNA fragments and to desalt the sample, the sample was passed through a C18 column (Dr. Maisch GmbH), followed by enrichment of the cross-linked peptides over an in TiO_2 column (GL Sciences) according to existing protocols[55] but using 10 μm TiO_2 beads as described previously.[21] The samples were subsequently dried, resuspended in 5% v/v acetonitrile and 1% v/v formic acid, and subjected to liquid chromatography and mass spectrometry analysis.

Analysis by mass spectrometry

A nanoliquid chromatography system (Dionex, Ultimate 3000, Thermo Fisher Scientific) coupled with a Q Exactive HF instrument (Thermo Fisher Scientific)[55] was used for liquid chromatography and mass spectrometry analysis. Online ESI-MS was performed in data-dependent mode using the TOP20 HCD method. All precursor and fragment ions were scanned in the Orbitrap, and the resulting spectra were measured with high accuracy (<5 ppm) at both the MS and MS/MS levels. A dedicated database search tool was used for data analysis.[69]

Promoter activity assay

The promoter region and 5′UTR of the CRISPR2 *cas* gene operon was PCR amplified using the primer pairs prom_*cas10*_luxAB_fw and prom_*cas10*_luxAB_rev to amplify the wild-type promoter and prom_*cas10*_mut_luxAB_fw and prom_*cas10*_luxAB_rev to substitute the ACAA motif in the conserved HLR1 site with a GGGG motif. For the CRISPR2 array promoter, we cloned the 100 base pair

region upstream of the transcription start site (positions 68274–68373) with the primers Prom_CRISPR2_fw and Prom_CRISPR2_RBS_rev to fuse the promoter with an artificial ribosome binding site.[82] The pILA backbone, containing a promoterless *luxAB* gene,[39] was amplified in three parts with the primer pairs pILA_1_fw (or pILA_1_RBS_fw for the CRISPR2 array promoter)/pILA_1_rev, pILA_2_fw/pILA_2_rev, and pILA_3_fw/pILA_3_rev. Primers were designed to overlap adjacent fragments. PCR fragments were assembled using AQUA cloning[83] and transformed into *E. coli* DH5alpha. The resulting plasmids were named pILA-$P_{CRISPR2\_cas10nat}$ and pILA-$P_{CRISPR2\_cas10mut}$, respectively. The constructs were subsequently transformed into an engineered *Synechocystis* 6803 strain, which carries the *luxCDE* operon encoding the enzymes for the synthesis of decanal.[79] Segregation of the constructs was achieved by transferring single clones to new BG11–0.75% Kobe Agar plates containing increasing concentrations of km (10–50 μg/mL). Full segregation was verified by PCR using the primers pIGA-fw and pIGA_rev and sequencing. The clones with segregated pILA constructs were grown in BG11 supplemented with 50 μg/μL km, 10 μg/μL chloramphenicol and 10 mM glucose under continuous light (30–50 μmol photons m^{-2} s^{-1}) with shaking until mid-logarithmic phase ($OD_{750\ nm}$ = 0.7–0.8). Cultures were diluted to $OD_{750\ nm}$ = 0.4 and incubated for 30 min prior to exposure to high-light conditions (300 μmol photons m^{-2} s^{-1}) for 4 h. Afterward, the cells were placed back in low light (40–50 μmol photons m^{-2} s^{-1}). As shown in Figure 2B, the cells were kept under high light after the initial 4 h of exposure and were not transferred back to low light. As shown in Figure 2C, DCMU was added to the cells during the high-light phase (at a final concentration of 50 μM). Bioluminescence was measured *in vivo* by using a VICTOR[3] multiplate reader (PerkinElmer) at total light counts per second. Cell suspensions (100 μL) were measured in a white 96-well plate (CulturePlate-96, PerkinElmer). Bioluminescence was measured before and after exposure to high light and every 30–60 min during recovery under low light. Next, we exposed the cells to both high and low light. On the basis of the results of preliminary tests, we noticed that the cellular production of decanal was not sufficient for monitoring bioluminescence *in vivo*. Therefore, we added 2 μL of decanal prior to the measurements. A strain carrying the promotorless *luxAB* gene served as a negative control. A strain carrying the P_{syr9}:*luxAB* construct was used as a control strain. Technical triplicates of biological triplicates were measured. Statistical relevance (details in Data S1) was calculated using a 2-tailed t test in Excel (Microsoft).

Electrophoretic mobility shift assay

For the binding of RpaB to wild type and mutated HLR1 motifs (Figure 2D), regions of interest were PCR-amplified from the respective pILA-PCRISPR2_*cas10* constructs using the primers EMSA_P*cas10*_HLR1_fw and EMSA_P*cas10*_HLR1_rev, which was labeled with Cyanine 3 (Cy3) at the 5′-end. The HLR1 motif from the *psbA2* promoter was used as a positive control and amplified using the primer pair EMSA_P*psbA2*_fw and EMSA_P*psbA2*_rev (Cy3 labeled). Different amounts of eluted 6×His-tagged RpaB (0–250 pmol) were mixed with 0.5 pmol of Cy3-labeled DNA target in binding buffer (20 mM HEPES-NaOH, pH 7.6; 40 mM KCl; 0.05 mg/mL BSA; 5% glycerol; 0.1 mM $MnCl_2$; 1 mM DTT; 0.05 μg/μL poly(dIdC)). The reaction mixture was incubated for 30 min at room temperature in the dark. Electrophoresis was performed in a 3% agarose-0.5 × TBE gel. The gel was run for 60 min in the dark at 80 V and 4°C. The signals were visualized with a Laser Scanner Typhoon FLA 9500 (GE Healthcare) using a green-light laser and Cy3 filter.

For Figure 4D, electrophoretic mobility shift assays were performed as follows: For transcript synthesis, a DNA fragment with coordinates 68373–68498 on pSYSA was amplified using the primers EMSA_CRISPR2LeadeR-T7_Fw (which carries a T7 promoter sequence followed by two Gs) and EMSA_CRISPR2LeadeR-T7_Rv. The resulting 128 nt transcript was labeled with Cy3. Binding of various amounts of purified recombinant His-tagged CrhR or $CrhR_{K57A}$ (ranging from 1 to 50 pmol) to 2 pmol (81 ng) of Cy3-labeled RNA was performed in buffer containing 20 mM HEPES-KOH (pH 8.3), 3 mM $MgCl_2$, 1 mM DTT, and 500 μg/mL BSA. As a substrate competitor, 1 μg of LightShift poly(dIdC) (Thermo Fisher Scientific) was added in high molar excess to the transcripts to confirm the specificity of the RNA–protein interaction. The reactions were incubated at room temperature for 15 min prior to loading on 2% agarose-TAE gels. The gel was run and the RNA visualized as for the Cy3-labeled DNA described above.

To test the performance of the various CrhR mutants in Figure S5, varying amounts (1–50 pmol) of purified recombinant His-tagged CrhR protein (WT or mutant enzymes) were mixed with 2 pmol of non-labeled transcripts (CRISPR2 leader or control). The binding assay was performed in 1 × buffer containing 20 mM HEPES-KOH (pH 8.3), 3 mM $MgCl_2$, 1 mM DTT, and 500 μg/mL BSA and in the presence of an excess of tRNAs as a competitor (tRNA for LightShift, Thermo Fisher Scientific) to address the specificity of the RNA/protein complex.

Reactions were incubated for 15 min at RT and then loaded onto a 2% agarose gel (in 0.5 × TBE). Gels were run for 1 h at 4°C and 80 V in 0.5 × TBE. Gels were stained with SYBR Gold (Thermo Fisher Scientific) for 15 min according to the manufacturer's instructions. Signals were detected using a Laser Scanner Typhoon FLA 9500 (GE Healthcare, now Cytiva) with the following settings: excitation, 473 nm; emission filter long pass blue ≥ 510 nm; photomultiplier value 400.

In vitro his-tag affinity purification and RNA pulldown

Recombinant proteins were isolated from *E. coli* M15[pREP4] strains via precipitation on Dynabeads magnetic beads (125 μL), which bind histidine-tagged proteins. To prove the coupling of His-tagged proteins to the beads, a 5% sample aliquot containing beads was washed after protein pulldown from *E. coli* M15 and used for SDS–PAGE analysis. The beads coupled with the His-tagged protein were further incubated in 25 mM Tris-HCl RNA elution buffer containing 2 M NaCl to eliminate contaminating RNA molecules from *E. coli*, washed in 1 × TBS, and incubated in the *Synechocystis* 6803 cell lysate for 20 min. RNA coprecipitated with the recombinant His-tagged proteins was eluted in the same RNA elution buffer and further utilized for the generation of libraries for Illumina sequencing.

Library preparation for RNA-seq

Total RNA was subjected to Turbo DNase (Thermo Fisher Scientific), purified, and size separated using an RNA Clean & Concentrator-5 Kit (Zymo Research) and treated with 5′-polyphosphatase (Epicentre) as described previously.[36] The RNA was 5′-phosphorylated by T4 polynucleotide kinase (NEB) and ligated to the 5′ adapter (Table S4). A ThermoScript Reverse Transcriptase Kit (Invitrogen) was used for cDNA synthesis, and the cDNA was amplified with Phusion High-Fidelity DNA polymerase (Thermo Fisher Scientific) using PCR_Primer_1 and PCR_Primer_2.1–2.10primers 1 and 2 (Table S4). The PCR conditions were 98°C for 30 s, followed by 18 cycles of denaturation at 98°C for 10 s, primer annealing at 60°C for 30 s, and extension for 15 s at 72°C, and a final extension step at 72°C for 2 min. The ExoSAP-IT PCR Product Cleanup Reagent (Thermo Fisher Scientific) was used for primer removal, and the samples were further purified with the NucleoSpin Gel and PCR Clean-up Kit and eluted with 20 μL of NE buffer. A 10 μL aliquot of each prepared DNA library was sequenced on an Illumina HiSeq 3000 sequencer as described.[36]

RNA-seq data analysis

RNA-seq data analysis was performed using tools installed in usegalaxy.eu. The paired-end or single-end reads were trimmed, and adapters and reads shorter than 14 nt were filtered out by Cutadapt 1.16.[84] Mapping was performed on the chromosome and plasmids of *Synechocystis* 6803 by Bowtie2 2.3.4.3 with the parameters for paired-end reads: -I 0 -X 500 –fr –no-mixed –no-discordant –very-sensitive.[52] Unmapped reads were filtered. Peak calling of the mapped reads was performed using PEAKachu 0.1.0.2[53] with the parameters –pairwise_replicates –norm_method deseq –mad_multiplier 2.0 –fc_cutoff 1 –padj_threshold 0.05.

QUANTIFICATION AND STATISTICAL ANALYSIS

Statistical analysis was performed with Excel Office 2019 (Microsoft). The measured bioluminescence of different *Synechocystis* strains exposed to different light conditions and chemicals were compared using a 2-tailed t test (Figures 2A–2C and 3D and Data S1). Differences between groups were considered to be significant at a p value <0.05.

Calculation of abundance of transcribed CRISPR2 RNA (Figures 5A and 5B) was done using Quantity One v4.6.6 (BioRad) using the volume analysis function.

Details of statistical analysis are summarized in Data S1.